FINNISH METEOROLOGICAL INSTITUTE
CONTRIBUTIONS

NO. 86

# HIGH-QUALITY POLAR UV MEASUREMENTS: SCIENTIFIC ANALYSES AND TRANSFER OF THE IRRADIANCE SCALE

Kaisa Lakkala

Department of Physical Sciences
Faculty of Science
University of Helsinki
Helsinki, Finland

ACADEMIC DISSERTATION in meteorology

To be presented, with the permission of the Faculty of Science of the University of Helsinki, for public critisism in Auditorium Physicum D101 (Gustaf Hällströmin katu 2) on December 10th, 2010, at 12 o'clock noon.

Finnish Meteorological Institute
Helsinki, 2010

ISBN 978-951-697-731-0 (paperback)
ISBN 978-951-697-732-7 (pdf)
ISSN 0782-6117

Yliopistopaino
Helsinki, 2010

FINNISH METEOROLOGICAL INSTITUTE

Published by Finnish Meteorological Institute
(Erik Palménin aukio 1) , P.O. Box 503
FIN-00101 Helsinki, Finland

Series title, number and report code of publication
Finnish Meteorological Institute
Contributions 86, FMI-CONT-86
Date
December 2010

Authors
Kaisa Lakkala

Title
# High-quality polar UV measurements: scientific analyses and transfer of the irradiance scale

Abstract

The Earth's ecosystems are protected from the dangerous part of the solar ultraviolet (UV) radiation by stratospheric ozone, which absorbs most of the harmful UV wavelengths. Severe depletion of stratospheric ozone has been observed in the Antarctic region, and to a lesser extent in the Arctic and midlatitudes. Concern about the effects of increasing UV radiation on human beings and the natural environment has led to ground based monitoring of UV radiation. In order to achieve high-quality UV time series for scientific analyses, proper quality control (QC) and quality assurance (QA) procedures have to be followed. In this work, practices of QC and QA are developed for Brewer spectroradiometers and NILU-UV multifilter radiometers, which measure in the Arctic and Antarctic regions, respectively. These practices are applicable to other UV instruments as well. The spectral features and the effect of different factors affecting UV radiation were studied for the spectral UV time series at Sodankylä.

The QA of the Finnish Meteorological Institute's (FMI) two Brewer spectroradiometers included daily maintenance, laboratory characterizations, the calculation of long-term spectral responsivity, data processing and quality assessment. New methods for the cosine correction, the temperature correction and the calculation of long-term changes of spectral responsivity were developed. Reconstructed UV irradiances were used as a QA tool for spectroradiometer data. The actual cosine correction factor was found to vary between 1.08-1.12 and 1.08-1.13. The temperature characterization showed a linear temperature dependence between the instrument's internal temperature and the photon counts per cycle. Both Brewers have participated in international spectroradiometer comparisons and have shown good stability. The differences between the Brewers and the portable reference spectroradiometer QASUME have been within 5% during 2002-2010. The features of the spectral UV radiation time series at Sodankylä were analysed for the time period 1990-2001. No statistically significant long-term changes in UV irradiances were found, and the results were strongly dependent on the time period studied. Ozone was the dominant factor affecting UV radiation during the springtime, whereas clouds played a more important role during the summertime.

During this work, the Antarctic NILU-UV multifilter radiometer network was established by the Instituto Nacional de Meteorogía (INM) as a joint Spanish-Argentinian-Finnish cooperation project. As part of this work, the QC/QA practices of the network were developed. They included training of the operators, daily maintenance, regular lamp tests and solar comparisons with the travelling reference instrument. Drifts of up to 35% in the sensitivity of the channels of the NILU-UV multifilter radiometers were found during the first four years of operation. This work emphasized the importance of proper QC/QA, including regular lamp tests, for the multifilter radiometers also. The effect of the drifts were corrected by a method scaling the site NILU-UV channels to those of the travelling reference NILU-UV. After correction, the mean ratios of erythemally-weighted UV dose rates measured during solar comparisons between the reference NILU-UV and the site NILU-UVs were 1.007±0.011 and 1.012±0.012 for Ushuaia and Marambio, respectively, when the solar zenith angle varied up to 80°. Solar comparisons between the NILU-UVs and spectroradiometers showed a ±5% difference near local noon time, which can be seen as proof of successful QC/QA procedures and transfer of irradiance scales. This work also showed that UV measurements made in the Arctic and Antarctic can be comparable with each other.

Publishing unit
Arctic Research, Climate Change

Classification (UDK)
551.501.6, 551.501.721, 551.508.25, 551.521.17
551.506.9

Keywords UV radiation, spectral irradiance, spectroradiometer, multifilter radiometer, quality assurance, QC/QA

ISSN and series title
0782-6117 Finnish Meteorological Institute Contributions

ISBN
978-951-697-731-0 (paperback), 978-951-697-732-7 (pdf)

Language
English

Sold by
Finnish Meteorological Institute / Library
P.O.Box 503, FIN-00101 Helsinki
Finland

Pages 156

Price

Note

ILMATIETEEN LAITOS

Julkaisija Ilmatieteen laitos, ( Erik Palménin aukio 1)
PL 503, 00101 Helsinki

Julkaisun sarja, numero ja raporttikoodi
Finnish Meteorological Institute
Contributions 86, FMI-CONT-86
Julkaisuaika
Joulukuu 2010

Tekijä(t)
Kaisa Lakkala

Nimeke
# UV-mittaukset napa-alueilla: tieteellinen analyysi ja irradianssiskaalan siirto

Tiivistelmä

Stratosfäärissä sijaitsevat otsonimolekyylit suojaavat maapallon ekosysteemejä auringon ultraviolettisäteilyn (UV-säteily) vaaralliselta osalta absorboimalla sen haitallisimpia aallonpituuksia. Voimakasta otsonimäärän vähenemistä on havaittu Etelämantereen alueen stratosfäärissä ja lievempää vähenemistä myös arktisilla alueilla ja keskileveysasteilla. Huoli lisääntyvän UV-säteilyn vaikutuksista luontoon ja ihmisiin on johtanut järjestelmällisten UV-säteilyn mittausten aloittamiseen. Korkealaatuiset tieteelliseen käyttöön soveltuvat UV-mittaukset vaativat järjestelmällisiä laadunvalvonta- ja laadunvarmistusmenetelmiä. Tässä työssä on kehitetty laadunvalvonta- ja laadunvarmistusmenetelmiä arktisilla alueilla mittaaville Brewer-spektroradiometreille ja Etelämantereen alueella mittaaville NILU-UV-monikaistaradiometreille. Menetelmiä voidaan soveltaa myös muille UV-mittalaitteille. Työssä on tutkittu myös Sodankylässä mitatun spektrisen UV-säteilyn aikasarjan ominaispiirteitä ja eri tekijöiden vaikutusta havaittuihin muutoksiin.

Ilmatieteen laitoksen kahden Brewer-spektroradiometrin laadunvarmistukseen kuuluvat päivittäinen ylläpito, laboratoriokarakterisoinnit, spektrisen vasteen laskeminen ja muutoksen seuraaminen, sekä mittaustulosten käsittely ja laadunarviointi. Tässä työssä on kehitetty uudet menetelmät mittaustulosten kosinikorjaukseen ja lämpötilariippuvuudesta aiheutuvan virheen korjaamiseen sekä mittalaitteiden spektrisen herkkyyden muuttumisen huomioimiseen. Uutta on myös rekonstruointimetelmällä laskettujen UV-säteilyn irradianssien käyttäminen mittaustulosten laadunvarmistuksessa. Mittaustulosten laskemisessa käytettyjen kosinikorjauskertoimien suuruudet vaihtelivat väleillä 1,08-1,12 ja 1,08-1,13. Lämpötilakarakterisointi osoitti lineaarisen riippuvuuden mittalaitteen sisäisen lämpötilan ja mitattujen fotonimäärien välillä. Molemmat Brewer-spektroradiometrit ovat osallistuneet kansainvälisiin vertailukampanjoihin, ja ne on todettu toiminnaltaan vakaiksi. Brewereiden ja kiertävän QASUME-vertailuspektroradiometrin mittaustulosten erot ovat olleet vuosina 2002-2010 korkeintaan noin 5 %. Sodankylässä mitatun spektrisen UV-säteilyn aikasarjan ominaispiirteitä on analysoitu vuosilta 1990-2001. Havaitut pitkäaikaiset muutokset eivät olleet tilastollisesti merkitseviä ja niiden suuruus riippui analysoidun ajanjakson pituudesta. Kokonaisotsonimäärä oli suurin UV-säteilyn muutoksiin vaikuttava tekijä keväisin, kun taas pilvisyydellä oli suurempi vaikutus kesäisin.

Tämän väitöskirjatyön aikana espanjalainen Instituto Nacional de Meteorogía (INM) perusti espanjalais-argentiinalais-suomalaisena yhteistyönä Etelämantereen alueelle NILU-UV-monikaistaradiometri -mittausverkoston. Tässä työssä on kehitetty kyseisen mittausverkoston laadunvalvonta- ja laadunvarmistusmenetelmiä. Ne sisältävät operaattoreiden koulutuksen, päivittäisen ylläpidon, säännölliset lamppumittaukset ja auringon UV-säteilyn mittausten vertailun kiertävän referenssiradiometrin mittauksiin. NILU-UV-monikaistaradiometreissä huomattiin jopa 35 % muutoksia kanavien herkkyyksissä neljän ensimmäisen toimintavuoden jälkeen. Tämän tuloksen pohjalta uutena tietona painotetaan säännöllisten lamppumittausten merkitystä myös monikaistaradiometreille. Kanavien herkkyyksien muuttuminen huomioitiin korjausmenetelmällä, joka perustui mittausaseman NILU-UV-radiometrin ja kiertävän referenssiradiometrin yksittäisten kanavien mittaustulosten keskinäiseen vertailuun. Korjauksen jälkeen asemien NILU-UV-radiometreillä ja referenssiradiometrilla mitattujen ihon punehtumisherkkyydellä painotettujen UV-annosnopeuksien keskimääräiset suhteet olivat 1,007±0,011 Ushuaiassa ja 1,012±0,012 Marambiossa, kun auringon zeniittikulma oli pienempi kuin 80°. NILU-UV-radiometreillä ja korkealaatuisilla spektroradiometreillä lähellä keskipäivää mitattujen UV-säteilyn irradianssien erot olivat ±5 %, mikä on osoitus onnistuneesta laadunvalvonnasta ja -varmistuksesta sekä onnistuneesta irradianssiskaalan siirrosta. Tämän työn tulokset osoittivat myös, että arktisten alueiden ja Etelämantereen alueiden UV-säteilyn mittaustuloksia voidaan vertailla keskenään.

Julkaisijayksikkö
Arktinen tutkimus, Ilmastonmuutos

Luokitus (UDK)
551.501.6, 551.501.721, 551.508.25, 551.521.17
551.506.9

Asiasanat
UV-säteily, spektrinen irradianssi, spektroradiometri, monikaistaradiometri, laadunvarmistus

ISSN ja avainnimike
0782-6117 Finnish Meteorological Institute Contributions

ISBN
978-951-697-731-0 (paperback), 978-951-697-732-7 (pdf)

Kieli
englanti

Myynti
Ilmatieteen laitos / Kirjasto
PL 503, 00101 Helsinki

Sivumäärä 156

Hinta

Lisätietoja

# PREFACE

The work included in this thesis has been done over the period 1999-2010 at the Finnish Meteorological Institute (FMI). I thank all those who acted as my overseers during that time period. I have belonged to two separate research groups, whose names have changed over the years, following the various organization changes at the FMI. My work tasks and closest colleagues have, however, remained unchanged, except that the persons in charge have changed. For giving me the opportunity to concentrate on my work, and for their understanding regarding the special arrangements made for family reasons, I am grateful to all the following: Esko Kyrö, Rigel Kivi and Kirsti Kauristie from the research groups at Sodankylä, and Petteri Taalas, Erkki Kyrölä, Juhani Damski, Aapo Tanskanen, Jussi Kaurola and Gerrit De Leuw from the research groups at Helsinki: thank you all!

My warm thanks is due to my supervisor, Esko Kyrö. I appreciate his professional skills and support. Whatever the subject, he has always been ready to help. I admire his enthusiasm for new ideas, and his open-minded outlook in developing the infrastructure of the FMI-Arctic Research Centre at Sodankylä. Thank you, Esko, for all these years!

I thank the preliminary examiners of this thesis, Germar Bernhard of Biospherical Instruments Inc. and Petri Kärhä of the Aalto University School of Science and Technology for their valuable comments. Hannu Savijärvi of the Division of Atmospheric Sciences at the University of Helsinki is acknowledged for his guidance and encouragement. I appreciate the work of Robin King regarding the language correction of this thesis.

The Antarctic NILU-UV network was established as a Spanish-Argentinian-Finnish co-operation task within the Spanish MAR project. I thank my colleagues from the Instituto Nacional de Meteorología, Emilio Cuevas, Alberto Redondas and Carlos Torres, from the Dirección Nacional del Antártico-Instituto Antártico Argentino, Hector Ochoa, and from the Centro Austral de Investigaciones Cientificas, Guillermo Deferrari and Susana Diaz, for our fruitful work done together. I also thank my colleague Outi Meinander for taking over the responsibility for the Antarctic UV duties of the FMI during my maternity leaves, as well as for all our work together.

Antti Aarva and the technicians of the former Observation Unit of the FMI are thanked for their help. I appreciate their skills in building the necessary equipment, as well as their helpful advice, which have been absolutely essential during the establishing of the first NILU-UV measurements at Ushuaia and Marambio.

The work with the Brewer spectroradiometer data would not have been possible without the help of my colleagues Hanne Suokanerva and Juha M. Karhu. I thank Markku Ahponen for carefully performing the lamp tests with the Brewer. The technicians at Sodankylä and Jokioinen are acknowledged for their help with the characterizations, and also for the pleasant times spent in the laboratories with them. I am

grateful to my colleague Tapani Koskela for sharing his knowledge of the Brewers, and for all his advice and help. I owe thanks to my deceased colleague Timo Turunen for introducing me to the computer world, as also to all the staff of the Arctic Research Centre at Sodankylä for their kindness and the unforgettable way they accepted me into their working community.

I wish to thank my colleagues and co-authors Antti Arola, Anu Heikkilä, Jussi Kaurola, Anders Lindfors and Aapo Tanskanen of the former UV group: I appreciate the opportunity we have had to work together. Without their help and support this work would not have been possible. I also thank Bjørn Johnsen of the Norwegian Radiation Protection Authority and my co-authors Arne Dahlback and Kåre Edvardsen for introducing me to the world of multi-band radiometers, as too my co-authors Julian Gröbner and Gregor Hülsen of the Physikalisch-Meteorogisches Observatorium Davos, World Radiation Center for their co-operation. I thank Leif Backman for his valuable help during the writing process of this dissertation. Since 2000, my workroom has been in the Aviation and Military Weather Service offices of the FMI at Rovaniemi. I thank all the staff there for giving me the opportunity to belong to their work community.

I thank my friends Laura Thölix and Terttu Leinonen for their friendship and support. Finally, I am grateful to my family: Timo, Eemil, Tuomas and Aapo.

This work has been financially supported by the European Communities DG XII under contract NO. ENV4-CT97-0540, the SCOUT-O3 and EDUCE projects, the Academy of Finland through the FARPOCC and SAARA projects and the Vilho, Yrjö and Kalle Väisälä Foundation. The Spanish MAR-project received financial support from the National R+D Plan of the Spanish Ministry of Science and Technology (National Research Program in the Antarctic) under contract REN2000-0245-C02-01.

Rovaniemi, October 2010
Kaisa Lakkala

# CONTENTS

# LIST OF ORIGINAL PUBLICATIONS


I Lakkala, K., Kyrö, E. and Turunen, T., 2003: Spectral UV measurements at Sodankylä during 1990-2001. *J. Geophys. Res.*, **108**, D199, 4621, doi:10.1029/2002JD003300.

II Arola A., Lakkala, K., Bais, A., Kaurola, J., Meleti, C. and Taalas, P., 2003: Factors affecting short- and long-term changes of spectral UV irradiance at two European stations. *J. Geophys. Res.*, **108**, D17, 4549, doi:10.1029/2003JD003447.

III Lakkala, K., Arola, A., Heikkilä, A., Kaurola, J., Koskela, T., Kyrö, E., Lindfors, A., Meinander, O., Tanskanen, A., Gröbner, J. and Hülsen, G., 2008: Quality assurance of the Brewer UV measurements in Finland. *Atmos. Chem. Phys.*, **8**, 3369-3383.

IV Lindfors, A., Kaurola, J., Arola, A., Koskela, T., Lakkala, K., Josefsson, W., Olseth, J. A. and Johnsen, B., 2007: A method for reconstruction of past UV radiation based on radiative transfer modeling: applied to four stations in northern Europe. *J. Geophys. Res.*, **112**, D23201, doi:10.1029/2007JD008454.

V Lakkala, K., Redondas, A., Meinander, O., Torres, C., Koskela, T., Cuevas, E., Taalas, P., Dahlback, A., Deferrari, G., Edvardsen, K. and Ochoa, H., 2005: Quality assurance of the solar UV network in the Antarctic. *J. Geophys. Res.*, **110**, D15101, doi:10.1029/2004JD005584.


In all the papers Kaisa Lakkala was responsible for the data processing and quality assurance of UV data measured by the Brewer spectroradiometer at Sodankylä and the NILU-UV radiometers at Ushuaia and Marambio. In papers I, III and V she was responsible for writing the manuscript, and in paper II she participated in writing the manuscript. In paper III, she was also in charge of the realization of the temperature and angular response characterizations of the Brewer at Sodankylä. As part of the work on paper V, she participated in establishing the Antarctic NILU-UV network, including the training of the operator at Ushuaia, and was authorized to negotiate the role of the FMI in the network. Papers II and IV, respectively, have also been included in the Doctoral Theses of Antti Arola (Arola, 2006) and Anders Lindfors (Lindfors, 2007).

# NOMENCLATURE

## LIST OF SYMBOLS

| | |
|---|---|
| $\theta$ | solar zenith angle |
| $\theta_0$ | solar zenith angle of the direct solar beam |
| $\lambda$ | wavelength |
| $\sigma(\lambda)$ | absorption cross-section |
| $\tau$ | vertical optical depth |
| $\tau_a$ | aerosol optical depth |
| $\tau_c$ | cloud optical depth |
| $\tau_r$ | Rayleigh scattering optical depth |
| $\tau_{O_3}$ | ozone optical depth |
| $\phi$ | azimuth angle |
| $\phi_0$ | azimuth angle of the direct solar beam |
| $\omega$ | solid angle |
| $\omega_0$ | single scattering albedo |
| $\Omega$ | total ozone |
| $a$ | surface albedo |
| $A$ | area |
| $a_i$ | coefficient in a linear equation |
| $c_i$ | scaling factor |
| $CMF$ | cloud modification factor |
| $CMF_{uv}$ | cloud modification factor of UV radiation |
| $CMF_g$ | cloud modification factor of global radiation |
| $E$ | irradiance |
| $E(\lambda)$,$E_\lambda$ | spectral irradiance |
| $E_{eff}$ | biologically-effective irradiance, dose rate |
| $E_{eff}(\lambda)$ | biologically-effective spectral irradiance, spectral dose rate |
| $E_{eff(cl)}$ | clear sky erythemally-weighted UV irradiance |
| $E_{eff(r)}$ | reconstructed erythemally-weighted UV irradiance |
| $E_M(\lambda)$ | measured spectral irradiance |
| $E_L(\lambda)$ | spectral irradiance of a calibration source |
| $E_s$ | scalar irradiance, actinic flux |
| $E_0$ | irradiance of the direct solar beam |
| $E_\infty$ | extraterrestrial irradiance |
| $H_{eff}$ | biologically-effective dose, dose |
| $I$,$I_0$ | intensity |
| $k$ | coverage factor |
| $k_i$ | instrument-dependent constant |
| $L$ | radiance |
| $L_\lambda$ | spectral radiance |

| | |
|---|---|
| $M$ | number of channels |
| $n$ | number density |
| $N$ | vertical column density |
| $P$ | scattering phase function |
| $R$ | unit radius |
| $r(\lambda)$ | spectral responsivity |
| $r'(\lambda)$ | relative spectral responsivity |
| $S(\lambda)$ | biological action spectrum |
| $S_L(\lambda)$ | signal of the radiometer when measuring a calibration source |
| $S_M(\lambda)$ | signal of the radiometer |
| $T$ | time |
| $V$ | voltage |
| $z$ | thickness |

# LIST OF ABBREVIATIONS

| | |
|---|---|
| AERONET | Aerosol Robotic Network |
| AOD | aerosol optical depth |
| CADIC | Centro Austral de Investigaciones Cientificas |
| CCD | charge-coupled device |
| CIE | Commission Internationale de l' Éclairage |
| DNA-IAA | Dirección Nacional del Antártico-Instituto Antártico Argentino |
| DXW | double-ended double-coiled (tungsten-halogen lamp) |
| EUVDB | European Database of UV radiation |
| FMI | Finnish Meteorological Institute |
| FUVIRC | Finnish Ultraviolet International Research Centre |
| HUT | Helsinki University of Technology |
| INM | Instituto Nacional de Meteorología |
| NILU | Norwegian Institute for Air Research |
| NIST | National Institute of Standards and Technology |
| NRPA | Norwegian Radiation Protection Authority |
| NSF | U.S. National Science Foundation |
| PAR | photosynthetically active radiation |
| PMOD/WRC | Physikalisch-Meteorogisches Observatorium Davos, World Radiation Center |
| PMT | photomultiplier tube |
| QA | quality assurance |
| QC | quality control |
| SP | Swedish Testing and Research Institute |
| SSA | single scattering albedo |
| SZA | solar zenith angle |
| TOMS | Total Ozone Mapping Spectroradiometer |
| USDA | United States Department of Agriculture |
| UV | ultraviolet |
| WHO | World Health Organization |
| WMO | World Meteorological Organization |
| WOUDC | World Ozone and Ultraviolet Radiation Data Centre |

# 1 INTRODUCTION

The Earth's ecosystems are protected from the dangerous part of the solar ultraviolet (UV) radiation by stratospheric ozone, which absorbs most of the harmful UV wavelengths. In the stratosphere, severe depletion of ozone has been observed, first in the Antarctic region (Farman et al., 1985), and later to a lesser extent in the Arctic and mid-latitudes. As the ozone in the atmosphere absorbs the short wavelengths of UV radiation, the amount of short-wavelength UV radiation was assumed to increase at the Earth's surface (WMO, 1990). The need for continuous surface UV radiation measurements became obvious.

Nowadays, the human effect on the global ozone amount has been recognized, and efforts to restrict the use of ozone-depleting substances have been made (WMO, 1999). The Montreal Protocol was established, and its restrictions have been successful in reducing the amount of substances depleting the stratospheric ozone layer (WMO, 2007). A recovery of the ozone layer is expected, signs of which are assumed to be detectable in the measured surface UV time series as decreased UV values (Andrady et al., 2009). In practice, the matter is not so simple, as changes in the surface UV radiation amount are also strongly dependent on changes in cloudiness, surface albedo and the aerosol content of the atmosphere. All these factors affecting UV are expected to be directly or indirectly affected by the possible climate change, e.g., via changes in the atmospheric temperature or humidity conditions.

The effect of changes in the stratospheric ozone layer should be especially noticeable at the ozone-induced cut-off part of the ultraviolet radiation spectrum, where the short wavelengths are most harmful for ecosystems (Young et al., 1993; UNEP, 1998, 2003, 2007). Monitoring these wavelengths is a big challenge, as the ozone absorption of UV radiation is strongly wavelength-dependent, and the dynamic range of the UV signal at these wavelengths is of several orders of magnitude. This means that even a small inaccurancy in the wavelength setting or in the detection sensivity of the spectroradiometer will result in erroneous data (Bernhard and Seckmeyer, 1999; Seckmeyer et al., 2001).

The key question and the most challenging part of the UV radiation measurements is the quality control (QC) and quality assurance (QA) of the data. This QC/QA includes daily maintenance, laboratory characterizations, corrections for all known measurement errors, and control of the homogeneity of the data time series (Webb et al., 1998, 2003). Only homogeneous time series allow the drawing of conclusions regarding long-term changes in the UV radiation amount. In this thesis, most of the work has been involved in ensuring the high quality of the bi-polar UV measurements (i.e., measurements in both the Arctic and Antarctic regions) of the Finnish Meteorological Institute (FMI), using both spectral UV radiometers and multi-band UV radiometers.

The FMI was among the first institutes to monitor UV radiation at high northern latitudes, in areas where spring-time polar stratospheric ozone loss was observed

(WMO, 1999; Bojkov et al., 1993; Kivi et al., 1999; Knudsen et al., 1998; Kyrö et al., 1992; Rex et al., 1997; Taalas et al., 1996). Spectral UV measurements were started in 1990 at the FMI Arctic Research Centre at Sodankylä. There, due to stratospheric dynamics, the natural variability in UV radiation is high, especially in springtime. The variability is enhanced by the influence of the ground snow cover, whose amount and duration vary from year to year. This combination, together with the possible chemical ozone loss, makes measurements at the site important from an ecological point of view. In springtime, at the start of the growing season, even small changes in the solar UV spectrum can be critical to the equilibrium of the ecosystem (Caldwell et al., 1980). Several studies of the impacts on nature of a possible enhancement of UV radiation have been conducted at Sodankylä (Turunen et al., 2002; Huttunen et al., 2005; Tiiva et al., 2007; Krywult et al., 2008; Rinnan et al., 2008; Haapala et al., 2009; Lappalainen et al., 2010; Martz et al., 2009).

Atmospheric conditions in Finland are challenging for UV measurements: e.g., most of the measurements are performed at a high solar zenith angle (SZA), most of the time the sky has changing cloud cover, and temperatures below freezing occur during wintertime. The work and experience of the FMI in successfully performing high-quality surface UV measurements under difficult atmospherical conditions led to international co-operation in establishing the Antarctic NILU-UV network. This network was founded in 1999 and 2000 as a Spanish-Argentinian-Finnish co-operation project. The bi-polar UV activities of the FMI became a part of the Finnish Antarctic project, and enable the comparison of surface UV measurements in areas of springtime ozone loss in both the southern and northern hemispheres.

The main objectives of this thesis have been: 1) to study the features of the spectral UV time series measured at Sodankylä, 2) to analyze the role of the different factors producing the observed UV features at Sodankylä, 3) to develop quality control and quality assurance practices that can be repeatable and suitable for many kinds of UV instruments, 4) to use measured spectral UV data and reconstructed UV calculations as quality assurance tools for each other, 5) to implement quality control and quality assurance procedures and guidelines in the Antarctic NILU-UV network and 6) to implement a travelling reference instrument to allow transfer of the UV irradiance scale between the Arctic and the Antarctic.

This thesis consists of five original papers, which will be referred to by roman numerals (I-V). The major contributions are as follows: PAPER I discusses the observed features of the spectral UV radiation time series at Sodankylä during the period 1990–2001. It gives a first approach to the dominant factors affecting the observed UV changes at Sodankylä. PAPER II gives a deeper analysis of the subject using, in addition to measurements, radiative transfer model calculations. The roles of the various different factors affecting UV radiation are assessed regarding both short- and long-term variations. In PAPER III the quality assurance of the two UV spectroradiometers at the FMI is discussed, including corrections for all known errors. New methods for characterizing and correcting errors due to temperature dependence and

non-ideal angular response are presented. Two methods are given to calculate the long-term change in the responsivity of the spectroradiometers. The complete data processing chain is explained, and is applicable to other spectroradiometers as well. As most of the ground-based UV measurements only started at the beginning of the 1990's, information about past UV levels has to be obtained in other ways. PAPER IV introduces a method based on available atmospheric parameters and radiative transfer calculations for the reconstruction of past UV radiation. The main idea is to use global radiation measurements for determining the influence of clouds on UV radiation. In PAPER V the quality assurance protocol of a multifilter NILU-UV-type radiometer network is set up and discussed. The quality assurance includes the transfer of the irradiance scale using a travelling reference instrument. This allows the comparison of measured UV radiation in areas of stratospheric ozone loss in both hemispheres.

This introductory review has the following structure: The theoretical background of UV radiation, UV measurements and the factors affecting UV radiation are given in Chapter 2. The three main types of ground-based UV measurement instruments are presented in Chapter 3. The main results are summarized in Chapter 4. The results are centred on the work done by the author of this thesis. In PAPER II, the focus has been on the time series at Sodankylä. The main contribution to PAPER IV is the use of ground-based data for the validation of reconstruction techniques. Chapter 5 concludes this thesis.

# 2 UV RADIATION IN THE ATMOSPHERE

As the focus of this thesis is the measurement of UV radiation, this theoretical part of the thesis will introduce the main body of knowledge about UV radiation, as well as the associated concepts and instruments. Section 2.1 introduces the geometrical definitions related to UV measurements, while sections 2.2 and 2.3 deal with the attenuation of solar UV radiation in the atmosphere and the related radiation transfer. The equations of those sections are reproduced from Madronich (1993). Section 2.4 discusses the main factors affecting the attenuation of UV radiation in the atmosphere. Often, the biological effectivity of UV radiation is the subject of interest. Biologically-weighted UV irradiances are the UV quantities mostly used in this thesis. The terminology describing biologically-active radiation is explained in section 2.5.

## 2.1 UV RADIATION AND GEOMETRY

In terms of energy, eight percent of the Sun's radiation reaching the Earth's atmosphere is UV radiation. It is energetic electromagnetic radiation, whose shorter wavelengths are biologically effective and would be harmful to the ecosystem if they reached the surface. However, atmospheric oxygen and ozone protect the Earth from the most dangerous wavelengths. The UV spectrum can be divided into different bands depending on their ozone absorption. The three longest UV wavelength parts are: 1) UV-C radiation (200–280 nm), which is totally absorbed by the atmosphere and does not reach the ground, 2) UV-B radiation (280–315 nm), which is strongly absorbed by the ozone layer and 3) UV-A radiation (315–400 nm), which reaches the surface and is least absorbed by ozone. The shorter wavelength part of the UV-B radiation band is the most harmful to the ecosystem. However, UV radiation can produce positive effects, e.g., via the cutaneous synthesis of pre-vitamin D (Webb et al., 1988; McKenzie et al., 2009).

The solar radiation reaching a target can be divided into three components: the direct solar beam, the diffuse part of the radiation and the reflected part of the radiation. Global radiation includes them all, while diffuse radiation includes all the radiation reaching the target, excluding the direct beam. Reflected radiation is radiation reflected from surfaces, most often below the target. The UV instruments discussed in this thesis measure global UV radiation. In practice, as the optical entrance of the UV instrument is usually looking upwards, the reflected component contributes via increased diffuse radiation from the sky. The characterization of the instruments, the understanding of the measurements, as well as the use of the radiative transfer calculations, all demand knowledge of the basic UV-related geometry. The basic geometrical components of UV radiation are presented in the next paragraphs.

The Sun can be regarded as a point source, which moves around the target. The angle between the local vertical and the solar beam is called the solar zenith angle, $\theta$, while the angle specifying the position of the Sun relative to South is the solar azimuth

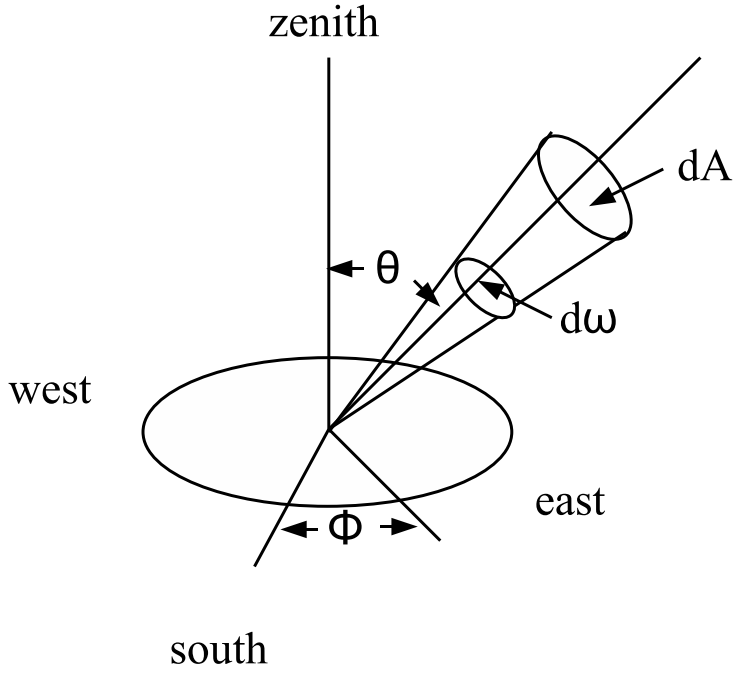


FIGURE 2.1. Definitions of azimuth ($\phi$), zenith ($\theta$) and differential solid angles ($d\omega$).

angle, $\phi$. The definitions are shown in Figure 2.1. Any direction in the sky can be expressed in terms of $\theta$ and $\phi$. The differential solid angle $d\omega$ centred on the direction $(\theta, \phi)$ is defined by the area element $dA$ on a sphere of unit radius ($R$), $d\omega = dA/R^2 = \sin\theta d\theta d\phi = d(\cos\theta)d\phi$. The total field of view is $4\pi$. Following Madronich (1993), the upper hemisphere with down-welling radiation and the lower hemisphere with up-welling radiation can be considered separately, each with $2\pi$ sr total field of view.

For a natural target, the total energy arriving from all directions can be calculated, if the radiance, $L(\theta, \phi)$, is known. The radiance is the energy arriving from the direction $(\theta, \phi)$ per unit solid angle, per unit area and per unit time on a plane perpendicular to the direction $(\theta, \phi)$. Its unit is $\mathrm{Wsr^{-1}m^{-2}}$. The energy intercepted by the target depends on the target shape and its orientation relative to the incoming radiation. Regarding biological effects, two idealized targets can be determined. If the target is a spherical surface, the total radiative power per unit cross-sectional area is the scalar irradiance or actinic flux

$$E_s \;=\; \int_0^{2\pi} \int_{-1}^{1} L(\theta, \phi)\, d(\cos\theta)\, d\phi. \tag{2.1}$$

The direct component can be separated from the diffuse component. $E_0$ is the irradiance of the direct solar beam incident at $\theta_0$ on a surface perpendicular to the beam. The upper and lower hemisphere can be considered separately, which yields two separate components accounting for the down-welling $L \downarrow (\theta, \phi)$ and up-welling

$L \uparrow (\theta, \phi)$ diffuse radiation. One obtains:

$$\begin{aligned} E_s &= E_0 + \int_0^{2\pi} \int_0^1 L \downarrow (\theta, \phi)\, d(\cos\theta)\, d\phi \\ &\quad + \int_0^{2\pi} \int_{-1}^0 L \uparrow (\theta, \phi)\, d(\cos\theta)\, d\phi. \end{aligned} \tag{2.2}$$

For a two-sided horizontal surface, the total radiative power received per unit area is simply the irradiance $E$, which can as well be divided into different components:

$$\begin{aligned} E &= \int_0^{2\pi} \int_{-1}^1 L(\theta, \phi) \cos\theta\, d(\cos\theta)\, d\phi \\ &= E_0 \cos\theta_0 + \int_0^{2\pi} \int_0^1 L \downarrow (\theta, \phi) \cos\theta\, d(\cos\theta)\, d\phi \\ &\quad + \int_0^{2\pi} \int_{-1}^0 L \uparrow (\theta, \phi) \cos\theta\, d(\cos\theta)\, d\phi. \end{aligned} \tag{2.3}$$

Both the radiance and the irradiance are integrated over wavelengths. They can also be defined as a function of wavelength $\lambda$, in which case they are the spectral radiance $L_\lambda$ and the spectral irradiance $E_\lambda$ with units $\mathrm{Wsr^{-1}m^{-2}nm^{-1}}$ and $\mathrm{Wm^{-2}nm^{-1}}$, respectively. The difference between the scalar irradiance and the irradiance is that the irradiance has a cosine factor to take into account the radiation coming from different directions to the horizontal surface. The units of both the scalar and the vector irradiance are $\mathrm{Wm^{-2}}$. As most UV instruments measure radiation arriving on a flat surface (diffuser), the irradiance $E$ is used. Most of the instruments are only sensitive to the radiation from the upper hemisphere and so the last term of the vector irradiance can be removed. However, the scalar irradiance would be more representative for organisms, as they are mostly randomly oriented, and receive radiation from all directions.

## 2.2 Absorption and scattering

Before radiation reaches the ground, it is attenuated by absorption and scattering processes in the atmosphere. When a UV photon is absorbed, it is completely removed from the radiation field. When radiation is scattered, the directions of the photons change from that of the direct solar beam simultaneously into various directions. Both scattering and absorption can be expressed by Beer-Lambert type expressions.

For absorption, the Beer-Lambert law can be described in the following way: Assuming monochromatic parallel radiation entering a horizontal layer of thickness $z$, the relationship between the incident intensity $I_0$ and the transmitted intensity $I$ is given by

$$I/I_0 = e^{-\tau(\lambda, z)/\cos\theta}, \tag{2.4}$$

where

$$\tau(\lambda, z) = \sigma(\lambda) n z \tag{2.5}$$

is the vertical optical depth (dimensionless) for absorption, and $\sigma(\lambda)$ is the absorption cross-section. The cross-section depends on the gas in question (e.g., ozone), and is a function of wavelength, possibly also of temperature and pressure. The absorbing gas is assumed to be uniformly distributed with number density $n$ , e.g., [molecules m$^{-3}$]. In the atmosphere, the gases are non-uniformly distributed, and the optical depth can be rewritten as

$$\tau(\lambda, z) = \sigma(\lambda)N, \tag{2.6}$$

where the vertical column density $N$ [molecules m$^{-2}$] is defined as

$$N \equiv \int n dz \tag{2.7}$$

In the case of scattering, an appropriate scattering cross-section is used, as well as the number densities of the particles and gases that produce the scattering. Photons can be scattered several times in the atmosphere. This is called multiple scattering, and is typical, e.g., in the presence of clouds and snow surfaces, where the radiation can be reflected back into the scattering radiation field. Scattering can be divided into Rayleigh scattering and Mie scattering, the former being valid for gases, and the latter for scattering by aerosols and cloud particles. In this thesis, the attenuation of UV radiation due to absorption and scattering by ozone, aerosols and cloud particles plays an important role in PAPER I, II and IV.

## 2.3 RADIATIVE TRANSFER

The Beer-Lambert law, presented in section 2.2, describes the monochromatic attenuation of the direct beam of solar radiation. Scattering processes also affect the diffuse part of the radiation field by increasing it. This is especially important at UV wavelengths, where Rayleigh scattering is dominant, and at all wavelengths if clouds and aerosols are present. According to Madronich (1993), for clear sky conditions, at 300 nm, 40 % to 100 % of the radiation can be diffuse, depending on the solar zenith angle. The proportion of diffuse radiation increases with increasing solar zenith angle. By contrast, in the visible wavelength range, most of the irradiance under clear skies, even at large solar zenith angles, is from the direct beam.

The radiative transfer of diffuse radiation is a complex problem, as the scattering of the atmosphere is not a straightforward process. Multiple scattering and interactions between different scatterers and absorbers make it complicated. The scattering directions, as well as the density distribution of scatterers and absorbers in the atmosphere, are not uniform. The ratio of the scattering efficiency to the total extinction is called the single scattering albedo $\omega_0$, and the scattering phase function $P$ is used to describe the angular distribution of the scattered radiation. $P(\theta, \phi; \theta', \phi')$ is defined as the probability that a photon incoming from a direction defined by the angles $\theta$' and $\phi$' will be scattered into angles $\theta$ and $\phi$.

In a plane-parallel atmosphere, using the single scattering albedo $\omega_0$ and the scattering phase function $P(\theta, \phi, \theta', \phi')$, the radiative transfer equation for diffuse radiance can be written, according to Madronich (1993), as

$$\begin{aligned} \cos\theta \, \frac{dL(\tau,\theta,\phi)}{d\tau} &= -L(\tau,\theta,\phi) + \frac{\omega_0}{4\pi} \, E_\infty \, e^{-\tau/\cos\theta_0} \, P(\theta,\phi;\theta_0,\phi_0) \\ &\quad + \frac{\omega_0}{4\pi} \int_0^{2\pi} \int_{-1}^{1} L(\tau,\theta',\phi') \, P(\theta,\phi;\theta',\phi') \, d\cos\theta' \, d\phi' \end{aligned} \quad (2.8)$$

where $\tau$ is the vertical coordinate measured in optical depth units and $E_\infty$ is the extraterrestrial irradiance. $\theta_0$ and $\phi_0$ are the angular coordinates of the direct solar beam. The first term on the right-hand side represents the attenuation of the radiance due to absorption and scattering. The second and third terms give the increase in the diffuse radiance due to scattering from the direct solar beam and the multiple scattering from other locations and directions, respectively. The sum of these terms must balance the vertical change in radiance, given on the left-hand side. Several numerical methods, more or less complex, have been developed to solve the equation.

The final result of the radiative transfer calculations is the spectral irradiance reaching the surface, $E(\lambda)$, which can be summarized as being the product of the extraterrestrial spectral solar irradiance $E_\infty$ and a wavelength-dependent effective atmospheric transmission function $T$. Considering the main factors affecting surface irradiance, $T$ can be expressed as a function of solar zenith angle, ozone optical depth $\tau_{O_3}$, Rayleigh scattering optical depth $\tau_r$, aerosol optical depth $\tau_a$, cloud optical depth $\tau_c$ and surface albedo $a$. The spectral surface irradiance can then be expressed as

$$E(\lambda) = E_\infty(\lambda) \, T(\lambda, \theta, \tau_{O_3}, \tau_r, \tau_a, \tau_c, a). \quad (2.9)$$

There are also other factors affecting the attenuation of the surface irradiance, such as absorption by other trace gases e.g., $NO_2$ and $SO_2$, and Raman scattering.

The different factors of the transmission function will be discussed in more detail in the next section (2.4). In PAPER II, the effects of the different factors of the transmission functions in producing the observed changes in the spectral UV irradiance were studied. There, the spectral irradiance reaching the surface was reconstructed using a radiative transfer model. The LibRadtran 0.15 package and 'UVspec disort' version were used (code is freely available from http://www.libradtran.org). In PAPER I, the effect of ozone absorption on the observed spectral UV changes at Sodankylä was also studied.

## 2.4 FACTORS AFFECTING UV RADIATION

The UV radiation entering the Earth's atmosphere is primarily controlled by the variations in the Sun's emittance and the orbital position of the Earth. As explained in section 2.3, the spectral UV irradiance reaching the surface can be expressed as the

product of the extraterrestrial irradiance and the transmission function (equation 2.9). The transmission function includes the absorption and scattering processes occurring in the atmosphere and at the surface. The main factors affecting the amount of UV radiation reaching the ground are: solar zenith angle, ozone, aerosols, clouds, surface albedo and the elevation of the measurement site. These factors will now be shortly introduced.

### *2.4.1 Solar zenith angle*

Depending on the solar zenith angle, the optical path of the radiation through the atmosphere can be shorter or longer, affecting both the absorption and scattering of the radiation. Due to these absorption and scattering processes, the wavelength distribution is affected, even though the greatest effect of the SZA is seen in the absolute values of UV radiation reaching the surface. The larger the SZA, the longer is the optical path, and the greater is the amount of radiation that is absorbed and scattered. This is detected as less radiation reaching the ground. The diffuse part of the radiation then increases. Thus, the relative contribution of diffuse and direct radiation to the measured UV irradiance generally depends on SZA.

The measurement capability of UV instruments can change with changing SZA. Measurements at large SZA are particularly challenging, as the diffuse part of the radiation field increases and the measured irradiance decreases. In such situations, the uncertainties in the measurements easily increase. One example is the uncertainty due to stray light at wavelengths shorter than 300 nm for single monochromator spectroradiometers (Bais et al., 1996). As the attenuation of irradiances is larger at short wavelengths than at longer wavelengths, following the shape of the ozone absorption spectrum, the relative influence of the stray light from longer wavelengths increases with SZA. As changes in SZA affect the wavelength distribution of the radiation, the results of solar comparisons between different instruments can change. This is the case, when comparing two broadband radiometers, if their spectral responses differ from each other.

### *2.4.2 Ozone*

Ozone ($O_3$) is formed naturally in the upper stratosphere above 30 km. There, the UV-C radiation at wavelengths shorter than around 240 nm is absorbed by oxygen molecules ($O_2$), which dissociate to give two oxygen (O) atoms, reaction 2.10. These free atoms combine with oxygen molecules to form ozone, reaction 2.11. When the solar UV radiation is absorbed by an ozone molecule, the energy is converted into heat, and the ozone molecule splits up into one oxygen molecule and one oxygen atom, reaction 2.12. Because reaction 2.11 is fast, ozone and atomic oxygen are quickly interconverted. Ozone can also be naturally destroyed by recombination of an ozone molecule and

an oxygen atom, reaction 2.13. The reactions 2.10 and 2.13 are slow, while reactions 2.11 and 2.12 are fast, and ozone is in local photochemical equilibrium in the upper stratosphere. These reactions are known as Chapman's reactions (Chapman, 1930).

$$\mathrm{O_2} + h\nu \rightarrow 2\mathrm{O} \qquad (\lambda < 242\ \mathrm{nm}) \qquad \text{creation of oxygen atoms} \qquad (2.10)$$

$$\mathrm{O} + \mathrm{O_2} + \mathrm{M} \rightarrow \mathrm{O_3} + \mathrm{M} \qquad \text{formation of ozone} \qquad (2.11)$$

$$\mathrm{O_3} + h\nu \rightarrow \mathrm{O_2} + \mathrm{O} \qquad \text{absorption of UV by ozone} \qquad (2.12)$$

$$\mathrm{O} + \mathrm{O_3} \rightarrow 2\mathrm{O_2} \qquad \text{recombination} \qquad (2.13)$$

Chapman's reactions represent the basic ozone cycle in the stratosphere, but do not explain the observed global distribution of ozone. The stratospheric circulation, the Brewer-Dobson circulation, and the chemical destruction of ozone have to be considered as well. In the Brewer-Dobson circulation, the air rises in the equatorial region and propagates toward the poles, carrying ozone with it. This explains the fact that even though more ozone is produced near the equator, the total ozone amount is higher near the poles. During the wintertime polar night, no ozone destruction occurs by photolysis, and ozone accumulates. This accumulation, taking place during the entire winter period, leads to a maximum in springtime. The natural annual cycle has its minimum in the autumn, when the stratospheric circulation is at its weakest and after photochemical reactions have been most effective throughout the summer.

Chemical ozone destruction includes ozone losses through catalytic reactions with hydrogen, nitrogen and halogen oxides. In these reactions a catalyst acts in the ozone destruction process, but is not consumed itself. For example, atomic chlorine, Cl, and chlorine monoxide, ClO, can catalyze the destruction of ozone by several mechanisms. The simplest is:

$$\mathrm{Cl} + \mathrm{O_3} \rightarrow \mathrm{ClO} + \mathrm{O_2} \qquad (2.14)$$

$$\mathrm{ClO} + \mathrm{O} \rightarrow \mathrm{Cl} + \mathrm{O_2} \qquad (2.15)$$

$$\text{Net effect:} \qquad \mathrm{O_3} + \mathrm{O} \rightarrow 2\mathrm{O_2} \qquad (2.16)$$

An ozone layer is formed in the stratophere between 10 km and 30 km resulting from the combined effect of the chemical production and destruction of ozone and the dynamics of the atmosphere. Within this layer, during the polar night when the temperature is low enough, polar stratospheric clouds can form. Chlorine-containing gases react on their surface, and when the sun appears during late winter / early spring, photolysis converts the gases into active chlorine radicals. These in turn effectively destroy ozone molecules via catalytic reactions. Bromine is known to play an important role in the chemical ozone-loss mechanism, and seems to be much more effective than chlorine. The Human effect on global ozone has been well assessed (WMO, 1999, 2007). Especially the polar latitudes of both hemispheres are affected, and severe springtime ozone loss has been detected in the Antarctic. The peak depletion occurs during the

spring of the southern hemisphere, when ozone is often completely destroyed over a range of altitudes. At some locations this can reduce the total ozone amount by two-thirds.

Ozone absorbs UV radiation effectively. Most of the UV radiation is absorbed at short wavelengths, with the absorption decreasing rapidly as a function of wavelength. The wavelength dependence of the ozone absorption of UV radiation has been studied and assessed in, e.g., Kerr and McElroy (1993), Madronich et al. (1995) and WMO (1999). Different spectral absorption cross-sections have been determined (Bass and Paur, 1984; Daumont et al., 1992; Molina and Molina, 1986). In a clear atmosphere, the ozone absorption at 280–300 nm together with Rayleigh scattering mostly affect the shape of the UV spectrum. The short wavelength cut-off is most sensitive to changes in the ozone column and the solar zenith angle.

About 10 % of all atmospheric ozone can be found in the troposphere, where local pollution sources can increase the ozone concentration. Madronich (1994) and Madronich and de Gruijl (1994) have introduced the radiation amplification factor (RAF) to link the changes of total ozone to the changes in biologically-active UV radiation. The RAFs depend on the altitude of the ozone perturbation. Brühl and Crutzen (1989) concluded that for given equal amounts, tropospheric ozone is a more effective UV-B absorber than stratospheric ozone for a high sun (SZA < 60°), but less effective for a low sun (SZA > 60°). The reason is that, for a high sun, the optical path length in the stratosphere is shorter and photons are more frequently scattered at a lower atmospheric level, leading to an amplification of tropospheric absorption. For a low sun, the effect is reversed: the optical path length in the stratosphere is longer, and more scattering and absorption can occur there before the radiation reaches the ground (Bernhard et al., 2003b).

### *2.4.3 Clouds*

Clouds and aerosols usually decrease the amount of UV radiation measured at the ground, while a bright surface with a high value of albedo increases it through the backscattering of reflected radiation. Bais et al. (1993) have determined by measurements that thick clouds can attenuate global solar UV radiation by as much as 80 % under an overcast sky at SZA 50°. den Outer et al. (2005) found that clouds, on average, reduced the daily erythemal dose by 68 % of the clear sky values in the Netherlands. Kylling et al. (2000) found that, relative to a cloudless sky, clouds reduce monthly erythemal doses by 20–40 % at Tromsø, Norway. Frederick and Lubin (1988) suggested that a thick cloud, in addition to its attenuation of UV radiation by obscuring the direct component, might cause an increase in the absorption by tropospheric ozone. This results from the scattering within thick clouds, which makes the downward radiation field more isotropic compared to clear-sky conditions, and thus the effective path length through tropospheric ozone longer.

It has been shown that scattered and broken clouds near the direction of the sun can act as reflecting surfaces for the direct solar beam, and occasional UV enhancement can be measured at the ground (Lubin and Frederick, 1991; WMO, 1999, 2003; Cede et al., 2002b). Sabburg and Wong (2000) made a one-year study, in which they found that 85 % of the UV-B enhancements occurred for solar zenith angles ranging from 40° to 63°. The maximum UV-B enhancement in irradiances was 8 % compared to a clear sky situation. They suggested that cloud-induced UV-B enhancement may be due to multiple scattering between different cloud layers. More recent studies show enhancement of up to 25 % (WMO, 2007).

The cloud modification factor ($CMF$) has been introduced to assess the influence of clouds on radiation (Calbó et al., 2005). The $CMF$ is defined as the ratio between the measured UV radiation under a cloudy sky and the calculated radiation for a cloudless sky. Typical $CMF$ values for overcast skies range from 0.3 to 0.8, depending both on the cloud type and its characteristics (Cede et al., 2002a; Calbó et al., 2005). Typically the $CMF$ of UV radiation differs from that of longer wavelengths (global radiation). Josefsson and Landelius (2000) reported that the cloud effect in the UV region is less than that for the whole solar spectrum. In PAPER IV, using radiative transfer calculations, a relationship was determined between the $CMF$ of global radiation and the $CMF$ of UV radiation. The $CMF$ for UV radiation was retrieved from a look-up table as a function of the solar zenith angle and the $CMF$ of global radiation, and used to reconstruct UV irradiances.

The wavelength dependence of the attenuation of UV radiation by clouds has been studied by Seckmeyer et al. (1996), Kylling et al. (1997), Bernhard et al. (2004), Winiecki and Frederick (2005) and Lindfors and Arola (2008). Kylling et al. (1997) and Bernhard et al. (2004) present two different physical explanations, whereas Lindfors and Arola (2008) assess the relative contribution of these two different physical effects to the total wavelength-dependent cloud effect in one specific case. Their results show that short wavelengths, in general, penetrate clouds more effectively than longer wavelengths, and that there are two important contributors to this wavelength-dependence: (1) that induced by multiple scattering between the cloud top and the atmosphere above and (2) that introduced by the wavelength-dependent radiance distribution at the cloud top together with the transmittance of the cloud alone as a function of angle of incidence.

### *2.4.4 Albedo*

The albedo expresses the reflection capability of a target. When talking about the albedo influencing UV radiation, the most common case is the surface albedo. Bright surfaces, like snow, ice or sand have a high albedo. Their presence increases the measured UV radiation compared to low albedo surfaces, like that of vegetation. A flat surface reflects radiation upward according to its albedo, and the enhancement in downwelling

radiation is due to the back-scattering of the atmosphere. In addition, the effect can be further enhanced in the presence of clouds, when the radiation is trapped between the cloud and the surface via multiple scattering and reflections.

Two types of albedo can be parametrized: local and regional albedo. The local albedo effect is seen via direct reflections, in which an area of approximatively a hundred metres in radius around the measurement place is calculated to have an effect. In the case of regional albedo, the effect of diffuse radiation also contributes, and in this case the radius of the affecting area can reach up to 40 km (Degünther et al., 1998).

During recent years, the albedo over snow surfaces has been of particular interest, as the snow and ice surfaces are expected to change due to the possible climate change. Measurements of snow albedo are still a big challenge due to the demanding measurement conditions as well as measurement uncertainties (Meinander et al., 2008). The UV albedo has been quantified over snow surfaces in the Antarctic (Grenfell et al., 1994; Smolskaia et al., 1999; Wuttke et al., 2006) and Arctic (Perovich et al., 2002; Meinander et al., 2008). The results show that the albedo of snow depends on the properties of the snow, and that the grain size of the snow differs between the European Arctic and Antarctic regions, which introduces a different UV albedo in these regions (Meinander et al., 2008).

Other atmospheric parameters, e.g., cloudiness and temperature, can influence the albedo. Wuttke et al. (2006) found that the UV zenith sky radiance can double due to the combined effect of clouds and a high snow albedo. The snow albedo can change within a few hours, due to the effect of temperature on snow's properties. Meinander et al. (2008) found that during one spring at Sodankylä, the midday erythemally-weighted UV albedo ranged from 0.6 to 0.8 during the accumulation period and from 0.5 to 0.7 during the melting period. The influence of the albedo on monthly erythemal doses at Tromsö has been studied by Kylling et al. (2000). They found that snow on the surface increases monthly erythemal doses by more than 20 %.

### *2.4.5 Aerosols and pollutants*

Aerosols are solid or liquid particles in the air; their typical size range is $10^{-9}$ m – $10^{-4}$ m. The presence of aerosols in the atmosphere affects both the radiation balance (Ardanuy et al., 1992) and the amount of UV radiation reaching the ground. The effect of aerosols on UV radiation can be direct via absorption and scattering (Coakley et al., 1983), semidirect via absorption that changes the cloud cover and liquid water path (Ackerman et al., 2000) and indirect via changing, e.g., the microphysics of clouds (Rosenfeld and Lensky, 1998). The UV reduction also depends on the vertical depth of the boundary layer, in which most of the aerosols are contained, and on the chemical composition of the aerosol particles.

The atmospheric loading of UV-absorbing and UV-scattering aerosols is the sum result of several sources of aerosols distributed over large areas by the atmospheric cir-

culation. Herman et al. (1997) have studied the aerosol loading measured by the Nimbus 7 Total Ozone Mapping Spectroradiometer (TOMS) for the years 1979–1993. They found that the major aerosol source regions are: (1) central South America (Brazil) near latitude 10°S; (2) Africa between latitudes 20°S–10°N; (3) the Sahara Desert and sub-Sahara region (Sahel), the Arabian Peninsula, and the northern border region of India; (4) agricultural burning in Indonesia, Eastern China, and Indochina, and near the mouth of the Amazon River; and (5) coal burning and dust in northern China. In addition to these, volcanic eruptions are important aerosol sources in the atmosphere.

Aerosol optical depth (AOD) is a columnar measure of the extinction, including both scattering and absorption of solar radiation by aerosols. The other properties needed to understand and model the UV radiative effects are the single scattering albedo (SSA) and the phase function. The SSA describes the amount of scattered and absorbed radiation, and it is the ratio of scattering to extinction. The aerosol phase function describes how much light is scattered in any direction. Both the SSA and the phase function can be retrieved from ground-based measurements (Petters et al., 2003; Santer et al., 2010). These measurements are still challenging, and many studies have been conducted to better understand aerosol measurements and aerosol's effects on UV radiation (WMO, 2007). Arola and Koskela (2004) have investigated, for instance, the various sources of errors in Brewer spectroradiometer AOD measurements. García et al. (2006) have studied the aerosol effect with data from the AERONET (Aerosol Robotic Network) and WOUDC (World Ozone and Ultraviolet Radiation Data Centre) databases, and Diaz et al. (2007) have reported the aerosol effect on spectral UV irradiance during a field campaign in Spain.

More about recent studies of UV-absorbing aerosols can be found in WMO (2007). Regarding satellite UV measurements, inappropriate handling of the aerosol absorption can be one of the reasons for the positive bias found when comparing these with ground-based UV measurements (Chubarova et al., 2002; Arola et al., 2005; Kazadzis et al., 2009). In order to correct this, Arola et al. (2009) have suggested a new approach to correct for absorbing aerosols in the UV.

In addition to tropospheric ozone, atmospheric pollution can reduce UV levels in local areas. Pollutant gases that absorb UV, such as $NO_2$ and $SO_2$, can reduce UV-B radiation by a few percent in heavily-polluted urban areas (Madronich, 1993). A list of pollutant gases absorbing UV radiation can be found in WMO (2007). Meleti et al. (2009) found that the improvement in air quality at Thessaloniki was the main reason for the observed increase in solar UV irradiance there.

### *2.4.6 Elevation*

The effect of the elevation of the surface above sea level is a complex question. The main phenomenon is that UV radiation increases with altitude, because of the shorter photon path through the atmosphere. The attenuation due to absorption and scattering

in the atmosphere is thus smaller than for longer photon paths. Most of the time, at high altitudes, snow increases the albedo as well as do clouds below the site, both of these resulting in enhanced UV radiation. Due to local conditions, such as atmospheric and surface parameters, the reported results are site-dependent, non-linear and vary with wavelength. Reported increases vary from 5 to 16 % per kilometre (Zaratti et al., 2003; Schmucki and Philipona, 2002; Pfeifer et al., 2006; Singh and Singh, 2004).

A concrete example of the effect of altitude can be found from the Lhasa region of Tibet, at 29° N. Dahlback et al. (2007), using NILU-UV multifilter radiometers, have measured the solar UV radiation in an altitude range of 3000 m to 5000 m during the winter and summer of 2003. They measured UV indexes that exceeded 15 on clear days. Values even higher than 20 were occasionally measured on partially cloudy days. The low total ozone values and clean atmosphere also contributed to these high UV values. Their study showed that for clear-sky and snow-free conditions, the increase in UV radiation was 7-8 % per km for erythemally-weighted UV dose rates.

## 2.5 BIOLOGICALLY-ACTIVE RADIATION

In this chapter, the common quantities used to express the biological activity of UV radiation are presented. They are often one of the last products of the UV data processing chain, and those that are distributed to the scientific community. This is the case for the spectral and multi-band UV data of the FMI, whose QC/QA processes are presented in PAPER III and PAPER V.

The sensitivity of organisms to UV radiation is strongly wavelength-dependent and depends on the effect studied. Different biological action spectra $S(\lambda)$ have been determined, and often the shortest wavelengths are the most effective. Examples of different action spectra are shown in Figure 2.2. These action spectra are used in the routine processing of the Sodankylä UV data. The CIE (Commission Internationale de l'Éclairage) erythema (McKinlay and Diffey, 1987), SCUP-H (de Gruijl and van der Leun, 1994) and Plant Damage (Caldwell et al., 1986) action spectra are shown. The product of the spectral irradiance and an action spectrum is called the biologically-effective spectral irradiance or the spectral dose rate $E_{eff}(\lambda)$. Its peak indicates the wavelength at which the biological effect is strongest. This peak is typically at wavelengths between 300 and 310 nm. For example, for the most well-known action spectrum, the CIE erythema action spectrum, which describes the wavelength dependence for causing sunburn, the strongest effect is at around 308 nm.

An estimation of the biological effect of the radiation over the wavelength range from $\lambda_1$ to $\lambda_2$ can be obtained by calculating the biologically-effective irradiance

$$E_{eff} = \int_{\lambda_1}^{\lambda_2} E(\lambda)\, S(\lambda) d\lambda. \tag{2.17}$$

The biologically-effective irradiance is also called the dose rate, the unit being $\mathrm{Wm}^{-2}$.

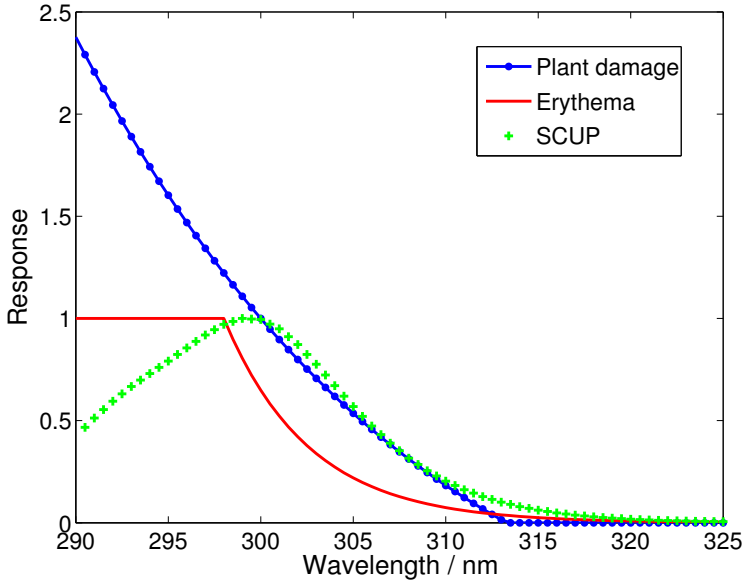


FIGURE 2.2. Examples of biological action spectra: a) CIE erythema, b) SCUP-H and c) Plant Damage. For explanation, see text.

In clear atmospheric conditions, the biologically-effective irradiances reach a maximum at any latitude at solar noon.

Broad-band UV instruments measure the dose rate directly. In this thesis, dose rates are also retrieved from the NILU-UV type multi-band radiometers (PAPER V). In the case of the FMI's NILU-UV radiometers, the UV dose rate can be calculated using the CIE erythemal and the Caldwell Plant damage action spectra. More about broad and multi-band instruments can be found in Chapter 3.

Integration of the biologically-effective irradiance over time from $T_1$ to $T_2$ gives the biologically-effective dose $H_{eff}$ accumulated over the period $T_2 - T_1$ as

$$H_{eff} = \int_{T_1}^{T_2} \int_{\lambda_1}^{\lambda_2} E(\lambda, T)\, S(\lambda)\, d\lambda\, dT. \tag{2.18}$$

The unit of $H_{eff}$ is $\mathrm{Jm}^{-2}$.

Nowadays, especially for public information, the use of the UV index has become popular. For the general public, this is a more comprehensible index than dose rates. It is a measure of the solar radiation at the Earth's surface, normally ranging from 0 to 16 at sea level. According to WMO (1994) and WMO (1997), the UV index is calculated by multiplying the CIE erythemally-weighted UV irradiance (McKinlay and Diffey, 1987) in $\mathrm{Wm}^{-2}$ by 40.

The World Health Organization (WHO) has made recommendations concerning protection against UV radiation. People are recommended to protect themselves when the UV index is over 3 (WHO, 2002). In Finland, the UV index is mostly within the

range from 1 to 6, reaching its maximum of 6 in the south of Finland during summer. At Sodankylä, in the northern part of Finland, the maximum UV index during the summer is around 5. A time series of the Sodankylä UV index measured with the Brewer spectroradiometer is shown in Chapter 4.

# 3 GROUND-BASED UV MEASUREMENTS

This thesis concentrates on UV radiation measured at the Earth's surface. Ground-based instrumentation is still the backbone of UV measurements, even though satellite retrievals and model calculations are becoming more and more accurate and common. Ground-based measurements are still the only ones that can instantaneously respond to rapid changes in cloudiness and other atmospheric conditions. When well-maintained and calibrated, ground-based measurements can reach an accuracy and repeatability of around 5 % (Gröbner et al., 2005). The errors are larger for model calculations, satellite retrievals and reconstructed UV time-series. The latter data sources are useful in areas or for time periods without ground-based measurements, as they can be used globally. Their validation, however, still relies on ground-based measurements.

UV measurement instruments can be divided into three main categories, depending on the wavelength resolution of the solar spectrum they monitor. Spectroradiometers are designed to monitor the whole spectrum with its fine structure, while broad-band and multi-band instruments have wider bandwidths. In the next sections 3.1–3.3, the different types of instruments are discussed in more detail, as well as their role in the FMI's UV measurement programme. As the work done in this thesis has concentrated on measurements made with spectroradiometers and multi-band radiometers, these instruments are described in more detail than the less-used broad-band radiometers.

The good accuracy of ground-based measurements can only be reached and maintained with careful monitoring and systematic quality control and quality assurance, including calibrations. The latter is an important part of UV data processing, and the calibration of the instruments is discussed in this chapter. The QC and QA procedures are discussed in more detail in Chapter 4.

## 3.1 SPECTRORADIOMETERS

Spectroradiometers measure the spectral irradiance as a function of wavelength. At UV wavelengths, one big challenge is the large dynamic range of five to six orders of magnitude of this part of the solar spectrum. A spectroradiometer can use a monochromator or a spectrograph to separate the wavelengths. In scanning spectroradiometers, like the Brewers, usually one grating is used to disperse the radiation from the entrance slit. Inside the instrument the optics focus the selected wavelength component on the exit slit. A photomultiplier tube (PMT) is typically used as detector. A spectroradiometer having only one monochromator is known to have stray light problems at UV-B wavelengths. The problem is reduced if two monochromators are used in tandem. Bais et al. (1996) reported stray light levels of $10^{-4}$ and $10^{-5}$–$10^{-6}$ relative to the maximum signal for a single and double monochromator Brewers, respectively.

Spectroradiometers measuring the entire spectrum simultaneously use a charged-coupled device (CCD) or a diode array detector. The advantage of this type of instru-

ment is that it records the spectrum continuously within a short time, e.g., 1 second, while scanning spectroradiometers usually require several minutes to scan a spectrum. The scanning time depends on the wavelength interval, bandwidth, step length and the time spent to measure at each position. This can lead to problems when interpreting the measurements, as the meteorological conditions and SZA change during a long scan. Ylianttila et al. (2005) reported a stray light level of $10^{-5}$ relative to the maximum signal after correction for a single monochromator diode array spectroradiometer.

The spectral irradiance $E_M(\lambda)$ can be calculated from the spectroradiometer signal $S_M(\lambda)$ as

$$E_M(\lambda) = \frac{S_M(\lambda)}{r(\lambda)}, \tag{3.1}$$

where $r(\lambda)$ is the spectral responsivity of the instrument. The spectral responsivity of the spectroradiometer is often determined by measuring a calibration source, usually a standard lamp. In practice, the measured irradiance $E_M(\lambda)$ will deviate from the "true" spectral irradiance $E(\lambda)$ owing to systematic and statistical errors.

Specifications for UV spectral instruments based on the objectives of UV research are given in Seckmeyer et al. (2001). There, two types of UV spectroradiometers, S-1 and S-2, are defined. Guidelines are given for instrument characterization, such as spectral responsivity, stray light determination, wavelength alignment, angular response and other parameters that influence the quality of the data. Bernhard and Seckmeyer (1999) have studied in detail the most common sources of errors of spectral UV measurements, which include radiometric calibration, cosine error, spectral resolution, wavelength misalignment, stability, noise, stray light and timing errors. They found that the expanded uncertainty, with a coverage factor $k$ =2, for global spectral irradiance measured with their spectroradiometer varied between 6.3 % in the UV-A and 12.7 % at 300 nm at SZA 60°. Garane et al. (2006) found the combined standard uncertainty ($\pm 1\sigma$) to be $\pm$4.8 % for their double monochromator Brewer, while for their single monochromator Brewer the uncertainty was $\pm$6.5 % at 305 nm and $\pm$5.3 % at 320 nm. Leszczynski (2002) reported expanded uncertainties ($k$ =2) of 5.6 % and 8.5 % for measurements of erythemally-weighted UV radiation performed with high-precision spectroradiometers.

The FMI uses Brewer spectrophotometers, manufactured by SCI-TEC, Canada, (Brewer, 1973; Bais et al., 1996). The measurements were started in 1990 at Sodankylä and in 1995 at Jokioinen. At Sodankylä there is a single monochromator Brewer, type MK II, serial number 037, which measures in the wavelength range of 290–325 nm. At Jokioinen there is a double monochromator Brewer, type MK III, serial number 107; its wavelength range is 286.5–365 nm. In addition to global UV irradiance, these instruments can also measure total ozone and the sulphur dioxide column. Both Brewers have a 35 mm diameter Teflon diffuser which is protected by a weather-proof quartz dome. The incoming light is directed through the foreoptics by director prisms. Monochromators have focusing lenses and diffraction gratings, and the detector used is a photomultiplier tube. Technical details of the Brewers can be found in SCI-TEC (1987), and

the instrument-specific details of the FMI Brewers can be found in PAPER III.

The QC and QA of UV measurements are discussed in detail in Webb et al. (1998) and Webb et al. (2003). For the spectral UV measurements of the FMI, the calibration, correction for known errors and other QC and QA procedures are discussed and documented in PAPER III. No uncertainty budget has been established for the FMI Brewers, but the quality assurance of the measurements is discussed using the inductive method described by Webb et al. (2003). There, the quality of measurements is evaluated using comparions with other independent spectral measurements.

The calibration of the spectroradiometers is based on lamp measurements. From these measurements, the spectral responsivity is determined as

$$r(\lambda) = \frac{S_L(\lambda)}{E_L(\lambda)}, \tag{3.2}$$

where $E_L(\lambda)$ is the spectral irradiance produced by the calibration source, and $S_L(\lambda)$ is the signal of the radiometer. Lamps are used to transfer an irradiance scale from an accredited calibration laboratory or national standards laboratory to the site spectroradiometer. In practice, this means that on-site calibration lamps are sent to the laboratory where the spectral irradiance of the lamps is determined. Back at the home site, these lamps are then used to transfer their calibration to working standards, which in turn are used to calibrate the spectroradiometer. For the FMI Brewers, 1000 W DXW lamps are used as known calibration sources. DXW-type lamps are double-ended double-coiled tungsten-halogen lamps. The signal of the Brewer is measured as photon counts per cycle, on the basis of which the unit of the spectral responsivity is counts(cycle)$^{-1}$s$^{-1}$(mWm$^{-2}$nm$^{-1}$)$^{-1}$.

Regular lamp measurements are needed in order to maintain the homogeneity of UV measurements. The calibration lamps themselves also need to be calibrated regularly, as their intensity may change with time. More than two lamps need to be used during a calibration to identify possible changes in the irradiance scale of the spectroradiometer. Three lamps give a better possibility of separating changes in lamp intensity from changes in the responsivity of the spectroradiometer. This procedure is explained in detail by Webb et al. (1998), while the practices followed by the FMI are discussed in PAPER III.

## 3.2 BROADBAND RADIOMETERS

Broadband radiometers are UV monitoring instruments that measure integrated irradiance over a large wavelength range. They can include both the UV-B and UV-A wavelengths of the solar spectrum, or they can cover only the UV-B or UV-A wavelengths. For solar UV measurements, the broadband radiometers have typically been designed to measure the irradiance weighted by the action spectrum for erythema as defined by the Commission International de L'Éclairage (CIE) (McKinlay and Diffey, 1987). Ideally, the spectral response of these broadband meters should resemble the

CIE action spectrum. In practice, the response functions of available instruments differ from the ideal function, and corrections, which typically depend on total ozone and SZA, become necessary.

Broadband radiometers are cheaper and easier to operate than spectroradiometers, and are thus suitable for remote locations and for networks including many instruments. They monitor with a higher time-resolution: data can typically be retrieved every minute, which makes them excellent for following rapid atmospheric changes. In this respect, broadband radiometers can provide complementary measurements to spectral UV measurements, whose measurement frequency is lower, and they can also be used as QC/QA tools (PAPER III). Broadband radiometers are good for providing data for information to the general public, such as the UV index.

Big challenges exist in the QC and QA of broadband radiometers (WMO, 2007; Seckmeyer et al., 2005): In order to be properly calibrated, the spectral and angular responses of the instruments need to be known. The measurements should also be corrected for known error sources. This is best achieved by combining simultaneous spectroradiometer measurements and model calculations. (Leszczynski, 2002) reported an expanded uncertainty ($k$ =2) of 7.8 % in the spectroradiometric calibration of erythemally-weighted radiometers in solar radiation. The calibration can also be transferred using a travelling reference (Blumthaler, 2004). However, the homogeneity of the UV time-series is difficult to ensure. The reason for this is that the instrument's responsivity can be affected by changes in the environmental conditions, such as changes in ambient temperature and humidity. In order to detect such effects, continuous monitoring of the responsivity is necessary, which is difficult to arrange. This limits the scientific use of the data, especially the interpretation of time series. However, broadband radiometers are practical for case-study-types of research, as they are portable and easy to set up.

The first broadband UV measurements at FMI were made with Solar Light 500 -type instruments at Jyväskylä and Jokioinen in 1991. Nowadays, the instrument type used is the Solar Light 501A (SL501A). First measurements with the SL501A were carried out at Helsinki in 1994, after which 5 more stations have been added: Sodankylä, Jokioinen, Sotkamo, Jyväskylä and Utö. The data are mostly used for information to the general public, but also as QC/QA tools (PAPER III) for spectroradiometer measurements and reconstructed UV time series (PAPER IV). As a QC tool, an SL501 radiometer is synchronized with the Brewer UV measurements at Sodankylä and Jokioinen. At every wavelength measured by the Brewer, the erythemally-weighted UV irradiance is recorded with the SL501A. This allows one to follow the effect of changing cloudiness, for example.

## 3.3 NARROWBAND MULTIFILTER RADIOMETERS

Narrowband multifilter radiometers (multi-band radiometers) measure solar radiation using several channels with bandwidths ranging typically from 2 to 10 nm. Usually they have 4 to 7 channels, where either a single channel or the combination of several channels give the desired information (Dahlback, 1996; Høiskar et al., 2003; Bernhard et al., 2005). Multifilter radiometers have the same advantages as broadband instruments: their price, around 20 000 euros, is lower than that of spectroradiometers, whose prices range from 50 000 euros up to even 150 000 euros. They are easier to operate and have no moving parts, and thus are easier to transport without affecting their calibration. They are designed to respond to the needs of scientific research and they monitor more diverse information than broadband radiometers. The use of empirical and radiative transfer model calculations together with their data allows calculation of secondary data products; for example, the following parameters can be retrieved from the NILU-UV type radiometer measurements: total ozone, UV-B irradiance, UV-A irradiance, UV dose rates weighted with different action spectra, cloud transmission and photosynthetically active radiation (PAR).

The calibration of the multifilter radiometer is based on simultaneous spectroradiometer measurements as well as on model calculations (Dahlback, 1996; Høiskar et al., 2003; Bernhard et al., 2005; Diaz et al., 2005). In order to retrieve accurate measurements, the relative spectral responsivity $r'(\lambda)$ for each channel $i$ has to be measured for each radiometer. Correction for the effect of ozone and SZA variation should be applied. Following Dahlback (1996), the voltage $V_i$ across the detector in channel $i$ that is due to illumination by radiation with spectral irradiance $E(\lambda)$ can be described by

$$V_i = \int_0^\infty r_i(\lambda) E(\lambda) \mathrm{d}\lambda, \tag{3.3}$$

where $r_i(\lambda)$ is the absolute spectral responsivity of channel $i$. The relation between the relative and absolute spectral responsivities can be written as $r_i(\lambda) = k_i r'_i(\lambda)$, where $k_i$ is a channel and instrument-dependent constant. The UV dose rate ($E_{eff}$) can be determined by a linear combination of the irradiances, represented by these voltages $V_i$, measured by the $M$ channels:

$$E_{eff} = \sum_{i=1}^{M} a_i V_i. \tag{3.4}$$

During the calibration a unique set of these $M$ coefficients $a_i$ is determined. A radiative transfer model is used to simulate dose rates representing different realistic atmospheric conditions, and the $a_i$'s are solved from a system of equations as presented in Dahlback (1996). For this, the constants $k_i$ need to be determined for every channel. This can be done using one spectroradiometer spectrum measured simultaneously with the radiometer measurement on a clear day near local noon.

The FMI has 4 NILU-UV6T multi-band radiometers obtained from the Norwegian Institute for Air Research (NILU), Kjeller, (Høiskar et al., 2003). Two of them are

continuously operated at Sodankylä at the Finnish Ultraviolet International Research Centre (FUVIRC). The third is used for snow albedo campaigns, and the fourth is the travelling reference of the Antarctic NILU-UV network. The NILU-UV radiometer has 5 UV channels, with central wavelengths around 305, 312, 320, 340 and 380 nm, and bandwidths of around 10 nm at full-width half-maximum. A combination of 3 to 5 channels is needed to retrieve the erythemally-weighted UV irradiance. The sixth channel measures PAR in the 400–700 nm wavelength region. The radiometer has a flat Teflon diffusor, and interference filters, and the radiation is recorded using silicon detectors. The instrument is temperature stabilized, and records data in a built-in data logger at a 1-min time resolution. Data with a 1-s time resolution can also be recorded.

UV-monitoring networks including multifilter instruments have been established by Norway (Mikkelborg et al., 2000), the U.S. National Science Foundation (NSF) (Bernhard et al., 2005), the United States Department of Agriculture (USDA) (Gao et al., 2010) and Greece (Bais et al., 2004). PAPER V presents the Antarctic NILU-UV multichannel radiometer network established by the Spanish-Finnish-Argentinian co-operation project. In PAPER V the quality assurance of a multifilter radiometer network is discussed in detail. It is emphasized that also these instruments need regular calibration, quality control and quality assurance in order to obtain reliable data. Høiskar et al. (2003) compared two weeks of erythemally-weighted UV dose rates measured under clear skies with a NILU-UV radiometer and a Bentham double monochromator spectroradiometer. The average ratio was $0.99 \pm 0.03$ for solar zenith angle up to $80^\circ$. Bernhard et al. (2005) found that, for UV-A irradiance, GUV multifilter radiometer and SUV-100 spectroradiometer data agree within $\pm$ 5 % for solar zenith angle up to $90^\circ$.

# 4 RESULTS

This chapter answers the six objectives of this thesis by summarizing the main results. In section 4.1, the observed features of the Sodankylä spectral UV time series are studied (objective 1) and the effects of the various different factors affecting UV radiation are assessed (objective 2). In section 4.2, the QC/QA procedures implemented for spectral UV measurements are introduced (objective 3). This section also shows the use of spectral UV measurements and reconstructed UV calculations as QA tools for each other (objective 4). The QC/QA procedures of the NILU-UV Antarctic network (objective 5) and the implementation of a travelling reference NILU-UV to transfer the required irradiance scale (obejctive 6) are discussed in section 4.3.

## 4.1 THE SODANKYLÄ SPECTRAL UV TIME SERIES

### *4.1.1 Observed features*

The Brewer spectrophotometer at Sodankylä was set up in 1988 in order to monitor the total ozone values at a polar site potentially vulnerable to Arctic ozone depletion. The instrument has a single monochromator and is, in addition, designed to make global spectral UV measurements in the wavelength range from 290 nm to 325 nm. The continuous UV measurement time series at this site started in 1989, which makes this spectral time series one of the longest in Europe. As part of this thesis, the UV time series has been re-evaluated and homogenized. This includes careful "detective" work, especially regarding the interpretation and use of the first years' calibrations. The UV time series have been homogenized using local lamp measurements, independent lamp measurements and international comparison campaigns. Despite this, it was not possible to ensure the quality of the UV data of the first year of operation: that year's data are unsuitable for scientific use. Details of the quality assurance and quality check of the Brewer UV data time series can be found in PAPER III, while its main results are shown in section 4.2.

In PAPER I, the homogenized time series is used to study the possible changes in the spectral UV time series at Sodankylä during the time period 1990–2001. During the mid-1990's, severe stratospheric ozone depletion was observed, and the need arose to study its effect on the spectral UV time series. As the effect of ozone depletion is expected to be seen at the short wavelengths of the UV spectrum, stringent requirements are placed on the instrumentation. Awareness of the stray light problem of single monochromators (Bais et al., 1996) caused the start of the wavelength range studied to be set at 300 nm, even when the stray light correction was used.

In order to study possible changes in spectral UV irradiances, a linear regression line was fitted to monthly mean irradiances for the wavelength range 300–325 nm in steps of 1 nm. The studied time period was each year from April to August in an SZA

interval from 63° to 65°. The Student $t$-test was used to study the statistical significance of the observed changes. The results are presented in Figure 4.1. The observed changes have been calculated and plotted for different time periods, varying the start and end year of the period. This demonstrates the influence of even a single year in such a short time series. More details of the analysis can be found in PAPER I, where the UV and total ozone time series studied can also be seen.

The conclusion drawn from the analysis was that the observed changes are strongly dependent on the chosen time period. For the whole time series, no statistically significant changes were observed, mainly because the variability in the UV irradiances was high and the time series studied was too short. The strong dependence on the time period studied was related to the severe ozone loss that occurred in the middle of the time period. In 1993, 1995, 1996 and 1997 there were cold Arctic winters, while in 1993, there was the additional effect of the Mount Pinatubo eruption, which increased the ozone depletion. As a result, the largest increase in UV irradiances was found in April for the period 1990–1997. At wavelengths shorter than 305 nm, the increase was over 15 % per year.

### *4.1.2 Factors affecting UV irradiance*

At Sodankylä, cloudiness plays an important role in UV measurements, as the sky is most of the time partly or totally covered by clouds. In PAPER I the effect of ozone has been separated from the effects of other atmospherical parameters, including cloudiness, using a statistical model. The global radiation measured with a pyranometer was used to represent the sky conditions. This was used together with total ozone values measured with the Brewer as input variables to the model. The analysis showed that changes in ozone and global radiation can explain most of the observed changes in the spectral UV irradiances at Sodankylä. Especially in April–May, ozone is the dominant factor at the shorter wavelengths, following the shape of the ozone absorption spectrum.

PAPER II studies a second way to assess the effects of the different factors affecting the observed UV changes. Radiative transfer model calculations have been used together with measured UV data. The same time series was used as in PAPER I, with the difference that in PAPER II the end year was 2000 and the studied SZA was normalized to 64°. The latter excluded the effect of a changing SZA, which was found to be important, even when the selected SZA band was only 2°. Ignoring that could have led to misinterpretation of the results. The influence of the different factors affecting UV was assessed regarding the short- and long-term changes in the spectral UV radiation.

The study was based on the assumption that the spectral surface UV radiation can be expressed using equation 2.9 (PAPER II). Considering only the main varying parameters, the spectral irradiance at any wavelength ($\lambda$) can be expressed as a function of SZA, ozone ($\Omega$), albedo ($a$), aerosol optical depth ($\tau_a$) and cloud optical depth ($\tau_c$),

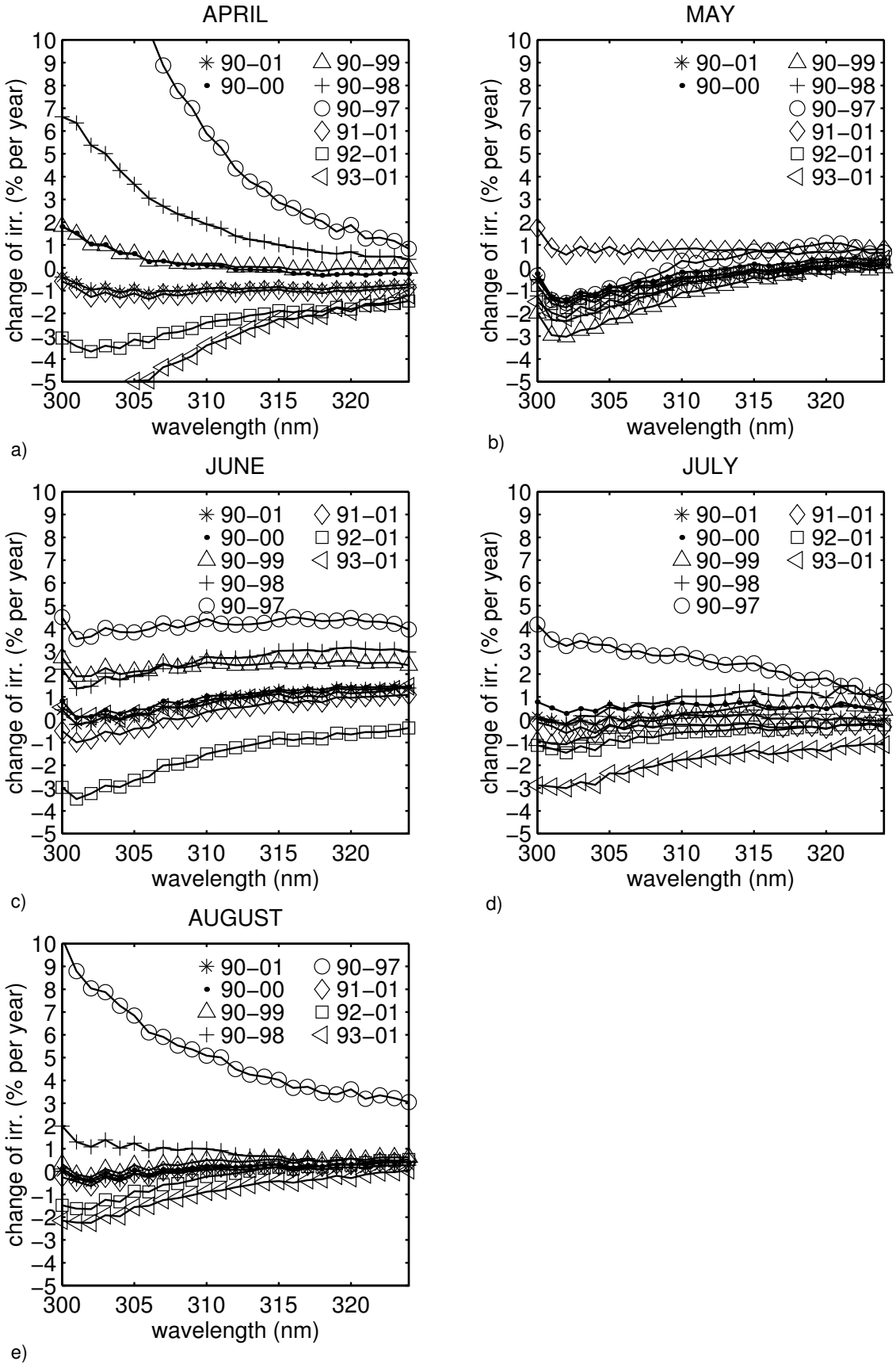


FIGURE 4.1. Relative changes (percent per year) in spectral UV irradiances calculated from linear regression lines fitted to different time periods during (a) April, (b) May, (c) June, (d) July and (e) August (from PAPER I).

i.e.,

$$E(\lambda) = f(\theta, \Omega, a, \tau_a, \tau_c). \tag{4.1}$$

Using this approach, the measured spectral UV time series were simulated using a radiative transfer model. In these simulations, environmental factors such as the Earth-Sun distance and the elevation of the site were given directly as input parameters to the model. Other optical properties, like the aerosol or cloud single scattering albedo and the aerosol or cloud assymmetry factor were also included as input parameters.

In order to study the effect of the different factors, daily climatologies of ozone ($\bar{\Omega}$), albedo ($\bar{a}$), aerosols ($\bar{\tau_a}$) and cloud effect ($\bar{\tau_c}$) were calculated for the period. These daily climatologies were used as inputs to the model, and the result represented the UV irradiance daily climatology $\bar{E}(\lambda)$. In order to estimate the influence of a single factor, that factor was allowed to vary as in reality. For example, the effect of ozone was studied in this way: the simulations of the UV irradiances (equation 4.1) were calculated using the daily climatologies of all the other input variables, but the ozone was allowed to vary as in reality. Equation (4.1) then becomes

$$E(\lambda) = f(\theta, \Omega, \bar{a}, \bar{\tau_a}, \bar{\tau_c}). \tag{4.2}$$

By comparing this model run to that made using only the daily climatologies $\bar{E}(\lambda) = f(\theta, \bar{\Omega}, \bar{a}, \bar{\tau_a}, \bar{\tau_c})$, the effect of ozone could be assessed. A more detailed description of the procedure can be found in PAPER II.

When studying the short-term effect, the maximum and minimum of the ratios $E(\lambda)/\bar{E}(\lambda)$ were calculated to estimate the greatest effect induced by the factor studied. The standard deviation of these ratios was used to represent the average effect. In April, the ozone-induced variability plays the most important role at short wavelengths. When studying monthly mean irradiances at 305 nm, the variability caused by ozone can be almost as high as 95 %, the average being about 35 %. For the summer months, the impact of cloud changes becomes stronger; the greatest changes in daily UV due to cloud variability were found to be about 200 %. The greatest variability induced in the monthly means was around 40 %, being on average 12 %. During spring time the albedo also had a strong enhancing effect, especially during May, which is often the snow melting period. The effect was around 20 %, when studying monthly means, being on average about 7 %. Aerosols played a minor role in explaining the UV irradiance variability at Sodankylä.

When studying the long-term variability caused by the different factors, irradiance time series were simulated using the model in a similar way to that used for studying the short-term variability. For example, to study the effect of ozone, the model was run using as input the actual ozone together with the daily climatologies of the other input variables (equation 4.2). In addition, the measured UV irradiance time series were reconstructed using the actual input data of equation 4.1. Instead of comparing these time series to daily climatologies, as in the short-term case, the long-term changes of each time series were investigated. The monthly means of the UV irradiances were

calculated. From these, changes relative to the means were calculated, and the Student $t$-test was used to find out whether the observed changes were statistically significant. As in PAPER I, total ozone was found to make a large contribution to the long-term UV variations at Sodankylä. The amplitudes of the variability induced by each factor in the time series were also calulated. The amplitude was defined as the [max-min]/mean of the irradiance values. Ozone induced the largest amplitude, 0.8, in monthly mean irradiances during spring-time. In this study, too, the time series were found to be too short for any trend detection.

## 4.2 QA OF BREWER MEASUREMENTS IN FINLAND

### *4.2.1 Characterizations and corrections*

Before using UV data in scientific research studies, such as PAPER I and PAPER II, the high quality of the data needs to be ensured. This can only be achieved by following appropriate, systematic quality control and quality assurance procedures. In PAPER III the QC/QA procedures for the two FMI Brewer spectroradiometers have been described in detail and the complete data processing chain has been presented. The data have been corrected with respect to known error sources using laboratory characterizations and theoretical approaches.

The signal of a spectroradiometer should be proportional to the cosine of the angle $\theta$ between the direction of the incident radiation and the normal of the radiometer's diffuser. This can be compared with the direct component of the solar irradiance measured on a horizontal surface in equation 2.3. The deviation from this ideal response is called the cosine error. PAPER III describes in detail the characterization of the angular response of the FMI Brewers. For the Brewer at Sodankylä, this was carried out three separate times in different laboratories and different years: 1996, 2000 and 2003. In 2000, the characterization was performed in the darkroom laboratory at Sodankylä, using a 1000 W DXW lamp. The lamp's irradiance was measured at various different incident angles at four different azimuth angles. The angular response obtained confirmed the characterization of 1996. At zenith angles larger than 50°, the cosine error of the direct beam exceeded 10 %. Using the angular responses and the new cosine correction method implemented in PAPER III, the actual cosine correction factors of the Brewers at Sodankylä and Jokioinen were calculated. These factors vary between 1.08–1.13 and 1.08–1.12, respectively, depending on the wavelength and the sky radiation distribution.

The temperature dependence of the Brewer UV measurements was characterized in the laboratories at Sodankylä and Jokioinen. The instrument was put into an insulated box, which was either warmed or cooled. The irradiance of a 1000 W working lamp was measured at different temperatures. The results of the measurements with the two Brewers showed a linear temperature dependence between the instruments' internal temperature and the photon counts per cycle. From the results, temperature coefficients

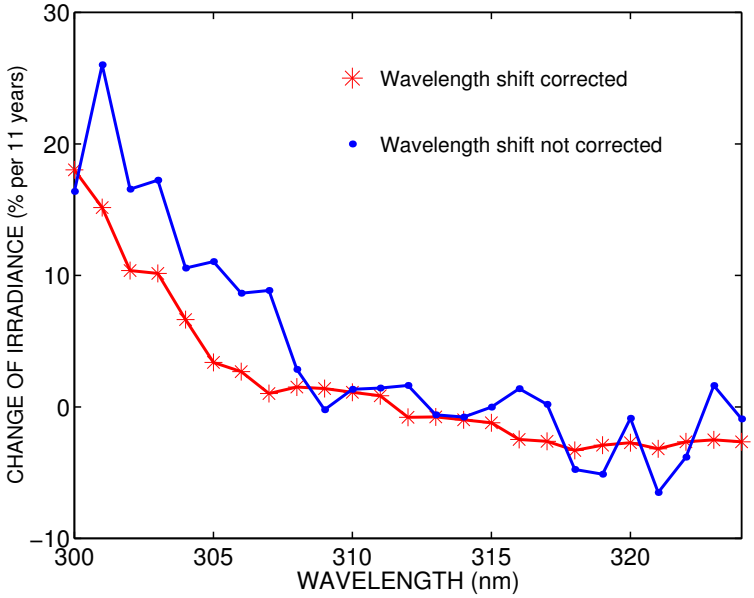


FIGURE 4.2. Relative changes (percent per 11 years) in spectral UV irradiances calculated from a linear regression line fitted to the April monthly means of 1990-2001 at Sodankylä.

were calculated. Using these coefficients, the measured irradiances are normalized to a reference temperature during the routine processing of the UV data. During a sunny summer day, a typical temperature correction to the measured irradiances is around 1 % at UV-B wavelengths for the Brewer at Sodankylä.

The slit functions have been measured and the wavelengths calibrated. The latter is an essential part of each annual maintenance. For the Sodankylä Brewer, a typical value for the wavelength shift at 305 nm before 1994 was -0.06 nm and 0.01 nm thereafter. This was calculated using the SHICRIVM wavelength shift correction package described in Slaper et al. (1995). Even though the values are relatively small, we found during the data analysis of PAPER II that this kind of stepwise change can be critical. If the wavelength error had not been corrected, the calculated long-term change of irradiances at some wavelengths could have been in error by 5-9 %. This is demonstrated in Figure 4.2, where the analysis of PAPER I has been reproduced using data for April which have not been corrected for the wavelength shift. The figure represents the observed UV irradiance change for the 11-year period 1990–2001.

The results obtained after correction of the wavelength errors of the Brewer UV measurements confirm the view that all known errors, however minor, need to be carefully studied and characterized. Generally, Brewer spectrophotometers are assumed to have only minor problems with wavelength alignment, and the wavelength shift correction could have easily been ignored with the shift values of lower than 0.1 nm that were found for the Sodankylä Brewer. In addition to the corrections for wavelength shift, temperature dependence and the cosine error of spectral irradiances, routine data processing includes corrections for all other known errors. This includes corrections of

errors due to noise spikes (Meinander et al., 2003), dark current, dead time and stray light. Details can be found in PAPER III.

When studying UV irradiance time series, it is important to be sure that the observed features are due to real variations in measured surface UV radiation and not caused by changes in the instrument's responsivity. The latter needs to be regularly monitored, in order to detect changes as quickly as possible, and to react to them by recalibrating the instrument. At Sodankylä and Jokioinen, the monitoring is done using 50 W and 1000 W lamp measurements every second week or monthly. Several lamps are used in order to separate the ageing of the lamps from the changes in the responsivity of the spectroradiometer. Special attention has been paid to detecting unsuccessful lamp measurements, as, e.g., even small irregularities in the current through the calibration lamp affect its spectrum.

1000 W DXW-type lamps, called calibration lamps, are used to transfer the required irradiance scale to the Brewer spectroradiometer. The irradiance scale used at FMI is based on the reference irradiance scale provided by the Helsinki University of Technology (HUT), which is the national standards laboratory for optical quantities in Finland (Kübarsepp et al., 2000). The primary standard lamps of the FMI are sent yearly to HUT for recalibration. The HUT irradiance scale is transferred to the other working lamps at FMI. The measurements of at least three of these calibration lamps are used to calculate the final spectral responsivity of the Brewer. This is demonstrated in Figure 4.3, where the Brewer responsivity at 305 nm is plotted during 2005 and 2006. The responsivities have been calculated from measurements of four lamps denoted d20, d22, d24 and d25. First, responsivities calculated from individual lamp measurements are plotted and bad measurements are excluded. Most often the responsivities, calculated with different lamps during the same day, agree with each other within 1 %, as in Figure 4.3. Next, one responsivity value for each day of the year has to be defined in order to get the responsivity time series. Two ways to calculate this final spectral responsivity have been presented in PAPER III. The one followed for the Sodankylä data consists of first averaging measurements on a given day, and thereafter performing a linear time interpolation between the days; finally, the small-scale time variations are smoothed by calculating a running average using a $\pm$ 15 day window. The black line in Figure 4.3 is the final responsivity for the years 2005 and 2006 at 305 nm. More about the spectral responsivity time series of the Brewers can be found in PAPER III. The responsivity of both Brewers have shown a downward drift of about two percent per year.

### *4.2.2 QA using reconstructed UV and intercomparisons*

Even after applying all known corrections and obtaining the proper spectral response, there can still be erroneous data points in the time series. Some checks are done "on the fly" during the data calculation process, e.g., unrealistic values are deleted; proper qual-

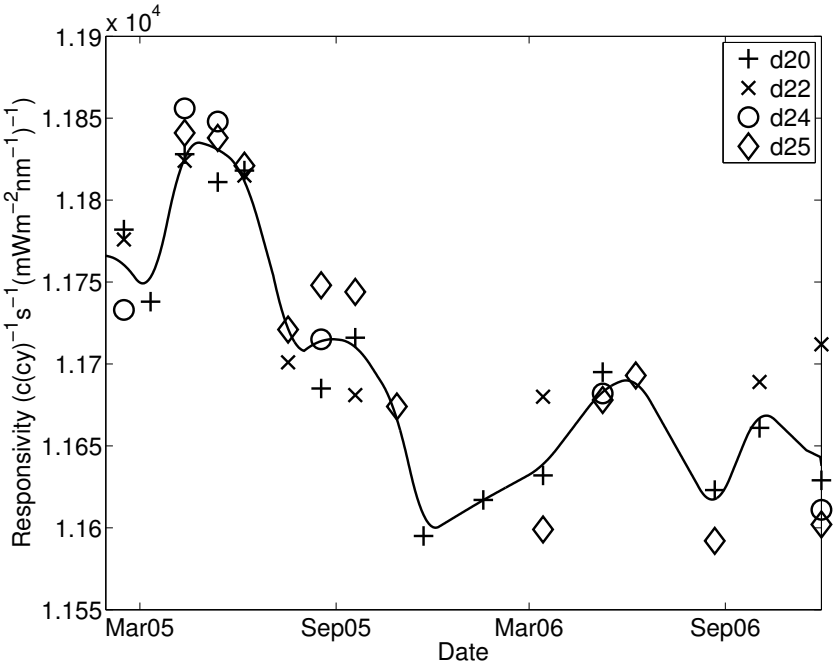


FIGURE 4.3. Responsivity of the Brewer spectroradiometer at Sodankylä at a wavelength of 305 nm measured with 4 different 1000 W lamps (d20, d22, d24 and d25) during 2005 and 2006. The black line is the final responsivity for the time period studied.

ity assurance of the final products is still needed, however. One possible way of doing this is to compare the measurements with model calculations or with other independent measurements (Webb et al., 2003).

In PAPER IV, erythemally-weighted UV irradiance time series were calculated using radiative transfer model calculations for the clear sky UV irradiance ($E_{eff(cl)}$) and the UV cloud modification factor ($CMF_{uv}$). The reconstructed UV irradiance can be expressed as $E_{eff(r)}$ = $E_{eff(cl)}\times$ $CMF_{uv}$ (PAPER IV). The CMF's of UV radiation ($CMF_{uv}$) are derived from a precalculated cloud modification table, which links the CMF of UV radiation to the CMF of global radiation ($CMF_g$) by the following relationship: $CMF_{uv}$=$f$($CMF_g$,$\theta$). Thus the method can be used in situations, where no UV radiation measurements exist, but for which global radiation measurements can be found. The CMF for global radiation can be found using the relationship of measured global radiation to calculated clear sky values. More details of the method can be found in PAPER IV; they are not discussed here further, as they have been presented in Lindfors (2007).

The method allows one to reconstruct UV time series for the past, before the start of ground-based UV measurements, if proper global radiation and ozone measurements exist. Reconstructed UV time series were calculated for Sodankylä for the time period 1983–2005. Linear trend analysis showed a statistically significant increase in UV

radiation of 4.1 %/decade at Sodankylä, mostly driven by a decrease in cloudiness.

During the development of the method, reconstructed UV irradiances were compared with ground-based Brewer spectrophotometer UV measurements, which served as validation tools for the method. The validation results are shown in detail in PAPER IV. During the process, some suspicious Brewer measurements were discovered; in this respect, the comparison served the other way round, as a QA tool for the Brewer measurements. In this case, erroneous Brewer UV measurements could be found. Thus it was realized that, in fact, comparisons of Brewer irradiances with reconstructed and modelled UV irradiances would be a good QA tool for spectral UV measurements. Comparisons with ancillary measurements, such as UV irradiances measured with SL501A radiometers and global radiation measured with CM-11 pyranometers, were also included. This QA tool was used to check the Sodankylä Brewer UV time series for every day for the period 1990-2007.

The modelled clear sky UV, the UV measured with the Brewer and SL501A instruments, and the reconstructed UV during one day are plotted in the same figure. Plots of the modelled clear sky global radiation and measured global radiation are also needed to confirm the result. If the plotted measurements differ from the reconstructed data, the other plotted parameters can give more information that helps to decide which is erroneous: measured or reconstructed. An example of a suspicious Brewer measurement is shown in Figure 4.4. On April 29, 2001, after an examination of the ancillary measurements, the Brewer measurements near 10:00 UTC were found to be erroneous.

In PAPER III, consideration is given to comparisons with other independent spectroradiometers performed as another QA tool. For the FMI Brewers, national comparisons are usually organized every second year. The Brewers have also participated in many international comparisons (Josefsson et al., 1994; Koskela et al., 1997; Gardiner and Kirsch, 1997; Bais et al., 2001; Thorseth et al., 2002). The campaigns, as well as their results, are reported in PAPER III. In the comparisons of the first years, many correction procedures were missing, such as cosine and temperature corrections, but during recent years all known corrections have been included. As one example of the stability of the performance of the Brewers, the comparisons with the international portable reference spectroradiometer QASUME from Physikalisch-Meteorogisches Observatorium Davos, World Radiation Center (PMOD/WRC) (Gröbner and Sperfeld, 2005) can be mentioned. The differences between the Brewers and the portable reference during the period 2002–2007 have been within 5 %, which can be taken as evidence of the good performance of the instruments. Similar differences were found during the latest comparison in May 2010.

Only after following the entire data processing chain, including quality control and quality assurance, can the data be distributed to the scientific community. The final spectral UV data of both Brewers at the FMI are submitted to the European Database of UV radiation (EUVDB), where they are freely available to scientists. All spectral data in this database undergo an automatic quality control procedure, and anomalies in the

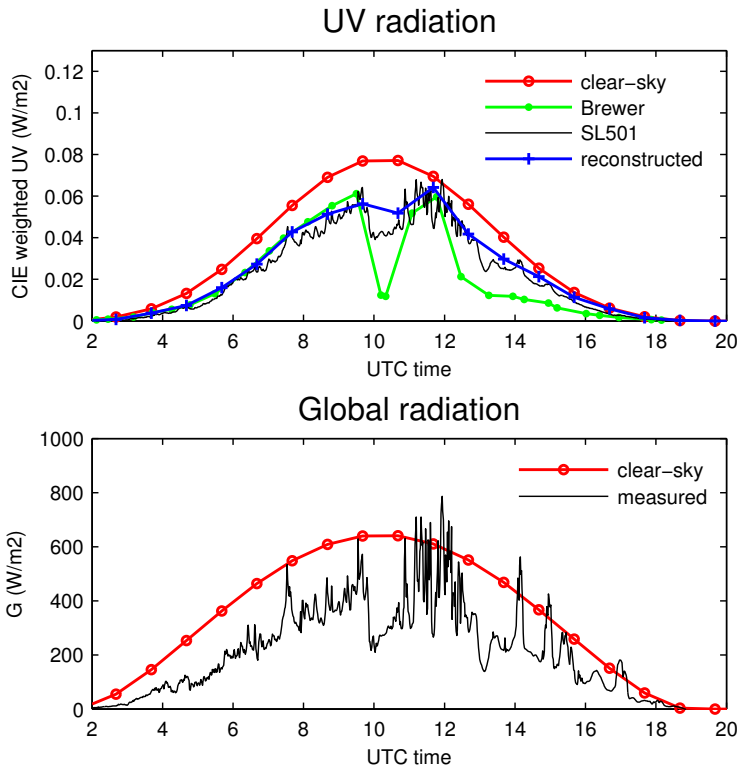


FIGURE 4.4. Brewer UV dose rates plotted together with modelled clear sky UV dose rates, reconstructed dose rates, SL501A dose rates, modelled clear sky global radiation and CM-11 pyranometer global radiation measurements at Sodankylä for 29 April 2001. (Figure 8 in PAPER III)

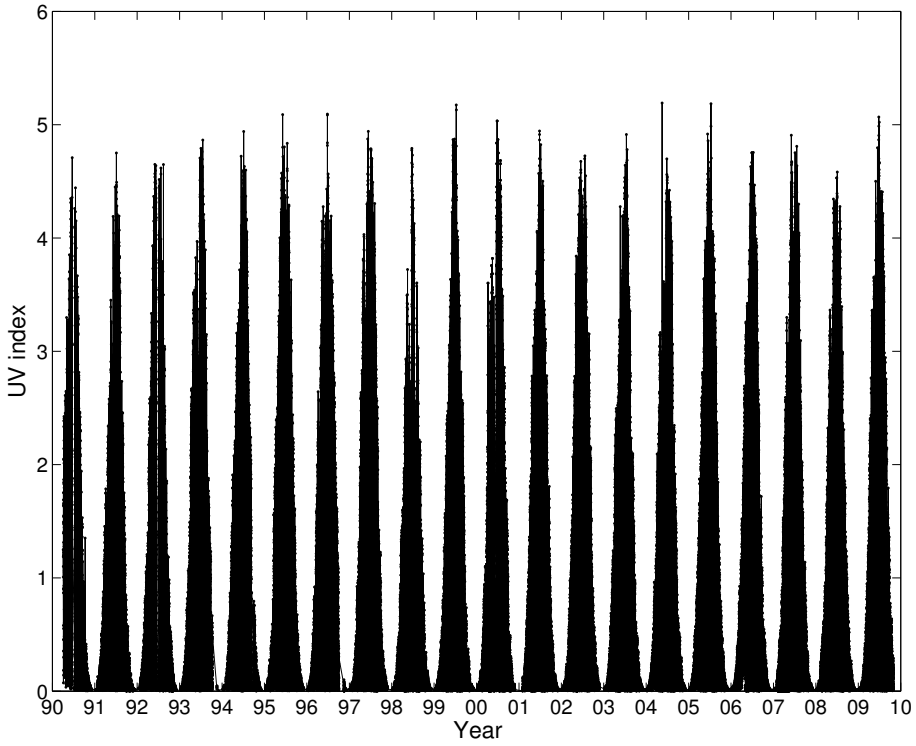


FIGURE 4.5. UV index time series calculated from all Brewer UV measurements during 1990–2009 at Sodankylä.

spectra from FMI are rarely found. As an example of the final product, the calculated UV index time series for Sodankylä, calculated from all the Brewer spectrophotometer measurements there, is presented in Figure 4.5 for the time period 1990-2009.

## 4.3 NILU-UV MEASUREMENTS IN THE ANTARCTIC

### *4.3.1 Implementation of the QC/QA procedures*

Even though the spring-time stratospheric ozone depletion was first noticed in the Antarctic, there are not many UV measurement sites in the area. There is, however, a need for ground-based UV measurements, as the satellite retrievals can still have inaccuracies of up to 50 %, especially at high latitudes and over highly reflecting snow or ice surfaces (Tanskanen et al., 2007). The task is not straightforward, as the climate conditions are difficult and most of the Antarctic area is uninhabited. The Spanish INM, Instituto Nacional de Meteorología, established a NILU-UV instrument network in 1999. The network has three stations, whose locations have been chosen to take into account the location of the stratospheric vortex. Belgrano II is mostly located inside the vortex, Marambio is at various times inside, on the edge of, or outside the vortex, while Ushuaia is mostly outside the vortex. The network is based on co-operation between the

INM, the Dirección Nacional del Antártico-Instituto Antártico Argentino (DNA-IAA), the Centro Austral de Investigaciones Cientificas (CADIC) and the FMI.

The role of the FMI is to provide a travelling reference NILU-UV multifilter radiometer and to maintain the stability of its irradiance scale. The FMI has played an important role in establishing the quality control and quality assurance procedures of the network, as it already has experience of high-quality UV measurements in harsh environmental conditions, in high northern latitudes. Guidelines for performing lamp tests and solar comparisons were established. The FMI helped to set up the first measurements and trained the operator at Ushuaia in December 1999. A defrost system, which was designed to blow warm air on the diffuser of the NILU-UV, was designed and built by the technical department of the FMI. The transport container of the travelling reference, which includes a complex lamp measurement system, was also constructed there. A mirror database has been established for the raw data and the QC/QA data of the network. All these activities have been done as part of the work for this thesis.

In PAPER V, the network and the QC/QA procedures are described in detail. One important part of the QC are the lamp tests, which are performed every second week at the stations. These tests allow detection of changes in the sensitivity of the channels of the instruments. In this case too, as for the FMI spectroradiometers (PAPER III), the use of more than two lamps is recommended in order to separate the ageing of the lamps from changes in the instrument responsivity. In the case of the NILU-UV instrument, which is designed to operate at a stable temperature, the heat of the lamp warmed the instrument 1-2°C during the lamp test and it needed around half an hour to cool. This created a practical problem at Ushuaia and Marambio, as tests with three lamps would have taken up too much of the operators' time. A compromise was agreed; to always use two lamps, but also a third lamp every third time.

After only 4 years of operation, drifts of up to -35 % were observed in the lamp test measurement time series of Ushuaia and Marambio. This was a surprise, as the multi-band radiometer had been assumed to be stable (Høiskar et al., 2003). The drifts observed at Ushuaia were linear, whereas at Marambio the drift of the first year started to recover during the following year. One suggestion was that moisture had entered the instrument and had then dried. These severe drifts in the sensitivity of the channels were in fact found to be due to optical degradation of the filters, a problem with the first NILU-UV instruments. An analysis of the lamp measurement results can be found in PAPER V.

As the UV dose rate retrieved from the instrument is a linear combination of each channel (equation 3.4), drifts in the channels will affect the UV dose rates and the total ozone values. The drifts therefore need to be detected as early as possible in order to correct the data. The options are: to recalibrate the instrument against a spectroradiometer (Dahlback, 1996), to correct for the drift of the channels by a correction factor (Redondas et al., 2008) or to transfer the calibration using a travelling reference (PAPER V). In the next section, and in PAPER V, the correction procedures of the UV

measurements of Ushuaia and Marambio are explained. In this case, the calibration is transferred using the travelling reference NILU-UV of the network, maintained by the FMI.

### *4.3.2 Transfer of the irradiance scale*

The QA of the network is based on a travelling reference multifilter radiometer, which visits Marambio twice a year and Ushuaia three times a year. On these visits, solar comparisons between the site NILU-UV and the travelling reference NILU-UV are performed. Using the results of these comparisons, the travelling reference is used to transfer the correct irradiance scale to the network and to ensure that the scale stays stable. A basic requirement is that the travelling reference has itself remained stable during the travels and over the years. This is checked by performing lamp tests before and after each solar comparison at the sites and in Finland. A set of lamps travels with the NILU-UV, but one set of 5–6 lamps stays at home, and these lamps are measured only once a year.

In order to avoid extra uncertainties caused by differences in measurement installations at various sites, travelling lamp test equipment has been built to accompany the reference NILU-UV in its container. A precision shunt resistor and a high-quality multimeter are included in the box, with all the cables already connected. When performing a lamp test, nothing has to be moved; only a current supply is needed from the site.

In order to assess the quality of the measurements, the travelling reference participates whenever possible in international solar comparisons (Thorseth et al., 2002; Meinander et al., 2004). The measurements are also compared with the other UV measurements on the site. For example, each time the reference instrument passes through Ushuaia its measurements are compared with those of the site's NILU-UV and the measurements of an SUV-100 spectroradiometer. The SUV-100 instrument is part of the NSF UV Monitoring Network, which carries out UV measurements at high latitude sites in Argentina, Antarctica and North America (Bernhard et al., 2010). Back in Finland, yearly comparisons are made either with the Brewer spectroradiometer at Jokioinen or at Sodankylä, or with both. Approximately every second year the travelling reference NILU-UV is sent to the manufacturer to be recalibrated against their reference instrument.

The solar comparisons allow checks to be made against the irradiance scales provided by different laboratories, and to estimate how successful the transfer to different sites has been. In this thesis, the calibration of the travelling reference NILU-UV was based on the scale provided by the manufacturer, which is traceable to the National Institute of Standards and Technology (NIST) via the laboratory of SP, the Swedish Testing and Research Institute (Johnsen et al., 2002). The scale of the SUV spectroradiometer of NSF was also traceable to NIST (Bernhard et al., 2003a), whereas the scales of the FMI Brewers were traceable to the irradiance scale provided by HUT.

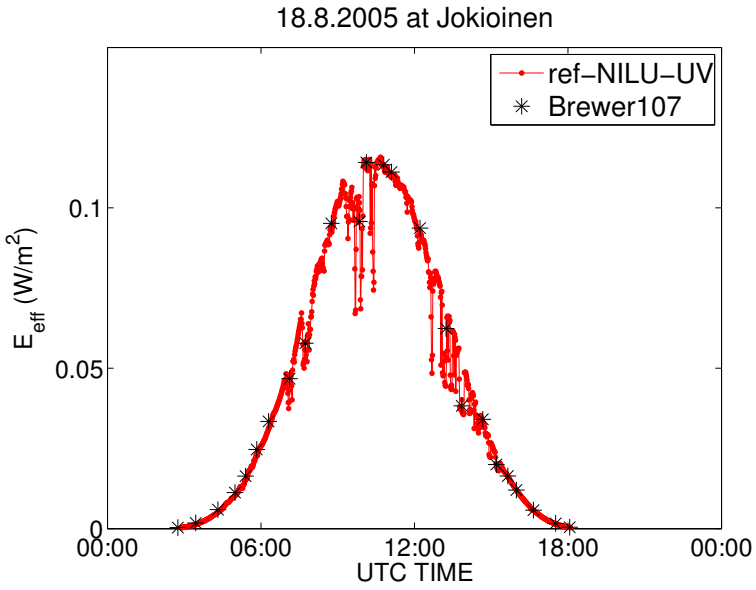


FIGURE 4.6. The erythemally-weighted UV dose rates measured with the travelling reference NILU-UV and the Brewer spectrophotometer at Jokioinen in 2005.

Figure 4.6 shows an example of a comparison between the travelling reference NILU-UV and the Brewer spectrophotometer at Jokioinen in 2005. The erythemally-weighted UV dose rates were compared. A clear sky moment near midday was chosen to represent the difference. On that particular day, the relative difference was around 1 % at an SZA of 48°. The relative differences of all comparisons performed between the NILU-UV and the Jokioinen Brewer during 2001–2005 are shown in Table 4.1. The results show that the relative differences with the Brewer spectroradiometer were within ±5 %.

Correspondingly, the results of the comparisons between the SUV spectroradiometer at Ushuaia and the travelling reference NILU-UV are shown in Table 4.2. A cosine correction of 5 % has been assumed for the SUV data (Bernhard, G., personal communication, 2004). As with the FMI Brewer, the relative differences of the erythemally-weighted UV dose rates were ±5 %. An example of a sunny comparison day is shown in Figure 4.7. For that day, the relative difference at an SZA of 48° was around 3 %. Figures 4.6 and 4.7 demonstrate the advantage of the NILU-UV multifilter radiometer compared to spectroradiometers. The NILU-UV can monitor UV radiation at time intervals of 1 minute, and in that way can react more rapidly to changes in atmospheric conditions.

The results presented above are valid for a clear sky and for measurements made near local noon. The SZA dependency of a comparison can be seen in Figure 4 of PAPER V, where the results of comparisons with the Sodankylä Brewer are shown. These comparison results show that the travelling reference NILU-UV agrees with the three spectroradiometers to within ±5 %, and thus the irradiance scales of the three

Table 4.1 The ratios of erythemally-weighted UV dose rates between the reference NILU-UV and the Brewer MK-III spectroradiometer at Jokioinen during 2001–2005. (Redondas et al., 2008).

| Date | SZA | Brewer/NILU-UV |
|---|---|---|
| 16.6.01 | 38 | 0.96 |
| 10.7.02 | 38 | 0.95 |
| 27.6.03 | 44 | 0.99 |
| 16.7.04 | 41 | 1.04 |
| 18.8.05 | 48 | 1.01 |

Table 4.2 The ratios of erythemally-weighted UV dose rates between the reference NILU-UV and the SUV-spectroradiometer during 1999–2006. Updated from PAPER V.

| Date | SZA | SUV/NILU-UV |
|---|---|---|
| 1.12.99 | 34 | 0.95 |
| 15.2.00 | 40 | 0.97 |
| 6.5.00 | 70 | 1.03 |
| 27.10.00 | 40 | 0.99 |
| 9.2.01 | 40 | 0.98 |
| 18.5.01 | 74 | 0.99 |
| 17.10.01 | 34 | 0.98 |
| 14.4.02 | 65 | 0.97 |
| 11.11.02 | 40 | 0.97 |
| 22.2.03 | 45 | 0.96 |
| 17.10.03 | 45 | 0.99 |
| 16.1.04 | 52 | 0.95 |
| 10.12.04 | 40 | 0.96 |
| 1.3.05 | 48 | 1.03 |
| 28.11.05 | 38 | 0.96 |
| 3.3.06 | 48 | 0.97 |
| 15.11.06 | 40 | 0.99 |

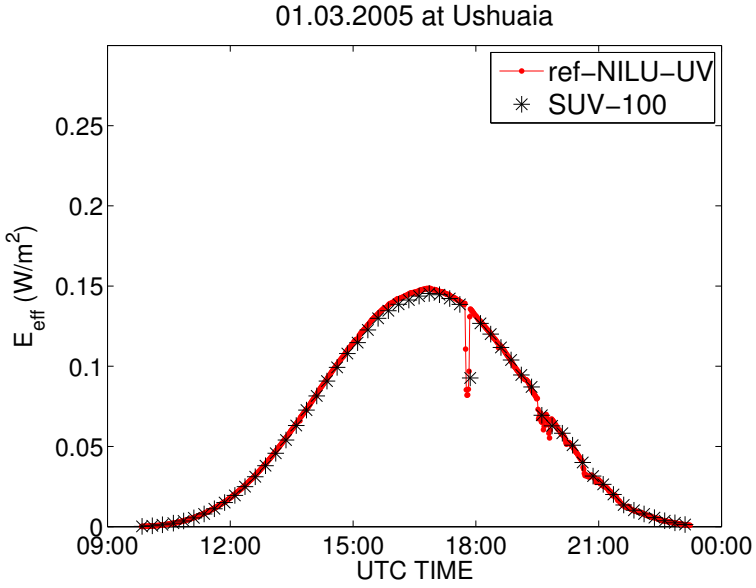


FIGURE 4.7. The erythemally-weighted UV dose rates measured with the travelling reference NILU-UV and the SUV spectroradiometer at Ushuaia in 2005.

different instrument types agree to within $\pm 5$ %. Considering the possible uncertainty factors in the calibration processes and irradiance scale transfer (Seckmeyer et al., 2001; Webb et al., 1998, 2003; Seckmeyer et al., 2005), and additionally the geographical distances between the two hemispheres, the results are encouraging.

The quality assessment by the solar comparisons discussed above, together with analyses of the lamp measurement time series, confirm that the travelling reference can be used to transfer the required irradiance scale to the NILU-UV radiometers at Ushuaia and Marambio. As stated earlier, during the first years of operation, the sensitivity of some channels of the NILU-UVs at Ushuaia and Marambio were found to decrease. PAPER V presents a method to correct the UV data. It shows that the effect of degradation of the filters, even by as much as 35 %, can be corrected. The restriction is that the filters of the instruments need to have nearly the same relative spectral response. Otherwise, the correction would become dependent on the effects of ozone and SZA variations (Diaz et al., 2005).

The method is based on raw data comparison of the travelling reference and the site instrument. Measurements are compared channel by channel, and a scaling factor is applied to the station's reading in order to make it match the travelling reference. Thus the erythemally-weighted UV dose rate of the site NILU-UV, $E_{eff(site)}$, can be calculated as

$$E_{eff(site)} = \sum_{i=1}^{5} a_i c_i V_{i,site}, \tag{4.3}$$

where $a_i$ is the coefficient of the linear combination of eq. 3.4 for channel $i$ of the

reference NILU-UV. $c_i$ is the scaling factor between the raw data of the site NILU-UV and the reference NILU-UV for channel $i$ and $V_{i,site}$ is the site NILU-UV raw signal voltage for channel $i$. Thus each channel of the site instrument is scaled to the corresponding channel of the reference instrument. More details about the calculation of the scaling factor can be found in PAPER V.

After the correction, the mean ratios of the erythemally-weighted UV dose rates measured during the solar comparisons in 2000-2003 between the reference NILU-UV and the site NILU-UV were 1.007 $\pm$0.011 and 1.012$\pm$0.012 for Ushuaia and Marambio, respectively, when the solar zenith angle varied up to 80°. This again confirms that the travelling reference can be used to transfer the established irradiance scale from one site to another, and can ensure that the measurements from different sites are comparable with each other. In our case, the travelling reference transferred the NIST-scale provided via the spectroradiometer of the Norwegian Radiation Protection Authority (NRPA) to the NILU-UV at Ushuaia and Marambio.

# 5 CONCLUSIONS

This thesis consists of five publications, in which six objectives are addressed.

The first objective was to study the features of the spectral UV radiation time series at Sodankylä. The second objective was to analyze the role of the different factors affecting the UV in this time series. The time series of Sodankylä is measured with one of the two well-maintained high-quality Brewer spectrophotometers at the FMI. The other instrument operates at Jokioinen; both of them have served the UV scientific community for more than 15 years (Gardiner and Kirsch, 1997; Bais et al., 2001; De Backer et al., 2001; Meinander et al., 2003; Lindfors et al., 2003; Glandorf et al., 2005; Gröbner et al., 2005; Huttunen et al., 2005; Kazantzidis et al., 2006; Meinander et al., 2006; Tanskanen et al., 2007; Krywult et al., 2008; Haapala et al., 2009; Lappalainen et al., 2010; Lindfors et al., 2009a,b; Martz et al., 2009; Seckmeyer et al., 2008).

The Sodankylä spectral time series is among the longest in Europe. It was analyzed in PAPER I and PAPER II for the time periods 1990–2001 and 1990–2000, respectively. In PAPER I the results were strongly dependent on the time period studied. This was demonstrated by varying the start and end years of the linear trend analysis. The biggest effect was seen in April, where an increase in irradiances of more than 10 % per year was found for the 1990–1997 time period at 305 nm. For the same wavelength the calculated change was -5 % per year for the 1993-2001 time period. Neither of the changes was statistically significant. In PAPER II, a new method including both observed UV measurements and radiative transfer model calculations was used to assess the effect of various factors affecting the short- and long-term UV changes. Both PAPER I and PAPER II confirmed that the time series studied were too short for trend analysis, which is also supported by Glandorf et al. (2005) and Weatherhead et al. (1998); ozone was found to be the dominant factor affecting UV radiation during the springtime at Sodankylä. For example, the years of high polar ozone loss in 1993, 1995, 1996 and 1997 caused anomalously high springtime UV irradiances. Clouds played a more important role in the observed UV changes during the summertime. The results of the analysis of the reconstructed UV time series in PAPER IV suggest a statistically significant increase of annual UV doses at Sodankylä for the period 1983–2005 that is mostly driven by decreased cloudiness. During the work done for these papers, it became obvious that the calculation of a linear trend over the whole available period is not always the best way to describe the observed features. The division of the year into different periods according to the atmospheric and climatic conditions was found useful, and in some cases a piecewise linear trend could be more informative.

In Europe, small increases in spectral UV irradiances have been reported using linear trend analysis. Zerefos (2002) studied the time series of Thessaloniki, Greece, with which our analysis can be compared. They found an increase of monthly mean UV irradiances at 305 nm of a couple of percent per decade, at SZA 63°, for the time period 1990–2001. For the same location, Meleti et al. (2009) found positive statistically

significant changes in UV irradiance of 5 % per decade at 305 nm during 1990–2005. The main reason for the observed increase was the improvement of air quality in Thessaloniki.

At the time of finalizing this thesis, it appears interesting to update the analyses of PAPER I and PAPER II. The recovery of the stratospheric ozone depletion is suggested to have started (Andrady et al., 2009; WMO, 2007) and it would be interesting to study possible signs seen in the Finnish UV time series. This update of the analysis will be the subject of work in the near future. Even if the effect of total ozone loss on UV is well reported, the spectral data are still interesting, e.g., they contain information on factors affected by climate change, such as cloudiness, aerosols and albedo. Possible changes in these factors affecting UV, together with changes in the interaction processes of the atmosphere, could possibly be seen in changes in the absolute values of UV radiation, as well as in the shape of the UV spectrum measured at the surface (McKenzie et al., 2007). For example: if, as a result of the climate change, the desert areas of the Sahara expand, more Sahara dust will be found in the atmosphere. These dust aerosols could directly influence the attenuation of UV via scattering and absorption processes, or they could act as condensation nuclei for clouds. The cloud amount and cloud properties could change, which would affect the amount of UV radiation reaching the surface, and possibly the wavelength distribution. Additionally, even though many studies have been made on the subject, there is still a lack of knowledge about the factors affecting UV radiation, such as aerosols and snow and ice albedos (WMO, 2007).

Besides supporting studies of the effect of stratospheric ozone depletion and climate change, the Finnish time series is interesting for validation of satellite-retrieved UV and reconstructed UV irradiances [Tanskanen et al. (2007); Lindfors et al. (2009b); PAPER IV]. Special features include the northern high latitude location with predominantly large SZA, winter snow, and rapidly-changing cloud conditions. Even if satellite, model and reconstruction-based UV data were to become more accurate, challenges under these kinds of conditions would remain. These data sets also have restrictions, such as low temporal and spatial resolution. High-quality ground-based measurements are essential for improving these kinds of UV retrieval methods. As the measurement conditions in Finland are also challenging for ground-based measurements, high-quality measurements can only be achieved if the QC/QA of these measurements is well planned and realized.

The third objective of this thesis was to develop quality control and quality assurance practices that would be suitable for many kinds of UV instruments. This is discussed in PAPER III, in which the QC/QA procedures of the Brewer spectroradiometers at the FMI were assessed. These procedures include daily maintenance, laboratory characterizations, calculation of long-term spectral responsivity, data processing and quality assessment. New methods for the cosine correction, the temperature correction and calculation of long-term changes in spectral responsivity were implemented. The results showed that the actual cosine correction factors of the Brewers at Sodankylä and Jokioinen can vary between 1.08–1.13 and 1.08–1.12, respectively, depending on the

sky radiance distribution and wavelength. The temperature characterization showed a linear temperature dependence between the instruments' internal temperature and the photon counts per cycle. The long-term spectral responsivity was calculated using the time series of several lamps, and it was scaled to the irradiance scale of HUT for the whole measurement time-period. The entire data processing chain from the raw signal to high-quality spectra was presented for the first time, and can be applicable to other instruments as well. The quality of the measurements was assessed by solar comparison with other independent instruments during international campaigns. Both Brewers have shown good stability. The differences between the Brewers and the portable reference spectroradiometer QASUME have been within 5 % during 2002–2010. Previous papers about the complete data processing procedure of spectral UV measurements have been published for the SUV-type spectroradiometers of the National Science Foundation network (Booth et al., 2001; Bernhard et al., 2004) and for the two Brewer spectrophotometers of the Aristotle University of Thessaloniki in Greece (Garane et al., 2006).

Interesting challenges still remain in correcting for known errors. The method presented in PAPER III for the cosine correction assumes that the diffuse radiation has an isotropic distribution. Actually the distribution is nonisotropic, and the handling of diffuse radiation in the cosine correction method could be investigated further. Also the stray light correction of the single monochromator Brewer could be improved. When comparing single and double monochromator Brewers, it seems that in some cases, e.g., at large SZA, stray light can still introduce errors of 2-3 % in measured irradiances at 305 nm. The uncertainty budget of the FMI spectroradiometers should be studied. The uncertainty budget of two Brewer spectroradiometers, one a single and the other a double monochromator, have been assessed in Garane et al. (2006), where they found combined standard uncertainties ($\pm 1$ $\sigma$) of 5-7 % for error sources affecting spectral UV measurements. This gives an idea of the possible total uncertainties of the Brewers at the FMI, but each Brewer has its own special characteristics, and the uncertainty budget needs to be determined for each instrument separately. As the single monochromator Brewer at Sodankylä is getting old, with over 20 years of monitoring to its credit, plans for ensuring the continuity of the valuable UV time series there should be made. A new spectroradiometer should be set up to measure for a couple of years before decommissioning the old one. This would ensure a long enough overlapping time period to guarantee the homogeneity of the data time series.

From the point of view of the data provider, most of the work is involved in quality assurance of the data. This is not seen by the public, often not even by the scientific community. It is obvious that proper QA is the foundation for achieving research-grade data. This work done in the QA field has shown that QA often seems endless: the more you study the data, the more you find new challenges. Sometimes it is worth thinking first, what accuracy level is needed in a particular study? For example, biological effect studies, satellite validations and climate change studies may each need a different accuracy level. PAPER III shows that wavelength shifts even smaller than 0.1 nm can

introduce errors of 5–9 % in trend studies. This is a good example of how the use of a data set for scientific purposes can uncover new knowledge about the effect of an error source, and in that way improve the correction and QA procedures.

The fourth objective of this thesis was to use measured spectral UV data and reconstructed UV calculations as mutual quality assurance tools. In PAPER IV a method based on available atmospheric parameters and radiative transfer calculations for reconstruction of past UV radiation was introduced. The main idea was to use global radiation measurements for determining the influence of clouds on UV radiation. As part of the work, the reconstructed UV irradiances were validated using the Brewer UV measurements at Sodankylä. During the study, anomalous Brewer spectra were found, and it became obvious that the roles can be reversed: The reconstructed UV can serve as a QA tool for ground-based measurements. To confirm a suspicion of anomalous spectral data, ancillary measurements such as broadband UV data and global radiation data measured with a pyranometer are needed, together with clear sky model calculations. This QA tool is explained in PAPER III.

The fifth objective of this thesis was to implement the QA/QC procedures and guidelines in the Antarctic NILU-UV network. The network was established in 1999-2000 as a Spanish-Argentinian-Finnish co-operation project. The FMI was asked to participate, as it had experience in performing UV measurements under challenging atmospheric conditions at high latitudes. I participated in starting the measurements and training the operator of the NILU-UV at Ushuaia. The QC/QA procedures were implemented and are described in PAPER V. They include daily maintenance, regular lamp tests and solar comparisons with the travelling reference instrument. Drifts of as much as 35 % in the sensitivity of the channels of the NILU-UV radiometers were found during the first 4 years of operation. This emphasized the fact that proper QC and QA are also needed for multi-band UV instruments. The uncertainty budget for the NILU-UV radiometers of the network should be determined in the future.

The sixth objective of this thesis was to implement a travelling reference instrument, enabling transfer of the irradiance scale between the Arctic and the Antarctic. In PAPER V, implementation of a suitable transfer method using a multichannel NILU-UV radiometer is discussed. Each site NILU-UV was scaled channel by channel to the travelling reference by performing solar comparisons. The method was found to be succesful, even though the differences between the raw data of the site NILU-UV and the reference instrument were, before the data correction, as much as 40 %. After the correction, the mean ratios of erythemally-weighted UV dose rates between the reference NILU-UV and the site NILU-UV were $1.007 \pm 0.011$ and $1.012 \pm 0.012$ for Ushuaia and Marambio, respectively, when the SZA varied up to 80°. The implementation of the method allows a comparison of the absolute UV values between different sites, and comparison of the effect of the stratospheric ozone depletion on UV radiation in the northern and southern hemispheres. The method is also applicable to other multichannel radiometer networks.

The travelling reference NILU-UV was compared with the SUV-100 spectrora-

diometer of NSF at Ushuaia and with the FMI Brewer spectrophotometers at Sodankylä and Jokioinen. The results showed that the relative differences near local noon time were $\pm 5$ %. This can be seen as an excellent result, and as proof of successful QC/QA procedures and transfer of irradiance scales. It proved that measurements made in the Arctic and the Antarctic can be compared with each other.

# REFERENCES

Ackerman, A. S., O. B. Toon, J. P. Taylor, D. W. Johnson, P. V. Hobbs, and R. J. Ferek, 2000: Effect of aerosols on cloud albedo: evaluation of Twomey's parametrization of cloud susceptibility using measurements of ship tracks. *J. Atmos. Sci.*, **57**, 2684–2695.

Andrady, A., P. J. Aucamp, A. F. Bais, C. L. Ballaré, L. O. Björn, J. F. Borman, M. Calwell, A. P. Cullen, D. J. Erickson, F. R. De Gruil, D.-F. Häder, M. Ilyas, G. Kulandaivelu, H. D. Kumar, J. Longstreth, R. L. McKenzie, M. Norval, N. Paul, H. H. Redhwi, R. C. Smith, K. R. Salomo, B. Sulzberger, Y. Takizawa, X. Tang, A. H. Teramura, A. Torikai, J. C. Van Der Leun, S. R. Wilson, R. C. Worrest, and R. Zepp, 2009: United Nations Environment Programme, Environmental Effects Assessment Panel, 2009, Environmental effects of ozone depletion and its interactions with climate change: progress report, 2008. *Photoch. Photobio. Sci.*, **8**, 13–22, doi:10.1039/b820432m.

Ardanuy, P., H. Kyle, and D. Hoyt, 1992: Global relationships among the Earth's radiation budget, cloudiness, volcanic aerosols, and surface temperature. *J. Climate*, **5**, 1120–1139.

Arola, A., 2006: *On the factors affecting short- and long-term UV variability*. Finnish Meteorological Institute, Contributions No. 54, Helsinki.

Arola, A., S. Kazadzis, N. Kotkov, A. Bais, J. Gröbner, and J. R. Herman, 2005: Assessment of TOMS UV bias due to absorbing aerosols. *J. Geophys. Res.*, **110**, D23211, doi:10.1029/2005JD005913.

Arola, A., S. Kazadzis, A. Lindfors, N. Krotkov, J. Kujanpää, J. Tamminen, A. Bais, A. di Sarra, J. M. Villaplana, C. Brogniez, A. M. Siani, M. Janouch, P. Weihs, A. Webb, T. Koskela, N. Kouremeti, D. Meloni, V. Buchard, F. Auriol, I. Ialongo, M. Staneck, S. Simic, A. Smedley, and S. Kinne, 2009: A new approach to correct for absorbing aerosols in OMI UV. *Geophys. Res. Lett.*, **36**, L22805, doi:10.1029/2009GL041137.

Arola, A. and T. Koskela, 2004: On the sources of bias in aerosol optical depth retrieval in the UV range. *J. Geophys. Res.*, **109**, D08209, doi:10.1029/2003JD004375.

Bais, A., C. Zerefos, E. Kosmidis, A. Kazantzidis, S. Kazadzis, and C. Topaloglou, 2004: Establishment of a network for UV monitoring in Greece. *Paper presented at Quadrennial Ozone Symposium, Int. Ozone Comm.*, 1-8 June, Kos, Greece.

Bais, A., C. Zerefos, and C. McElroy, 1996: Solar UVB measurements with the double- and single-monochromator Brewer Ozone Spectrophotometers. *Geophys. Res. Lett.*, **23**, 833–836.

Bais, A., C. Zerefos, C. Meleti, I. Ziomas, and K. Tourpali, 1993: Spectral measurements of solar radiation and its relation to total ozone, $SO_2$ and clouds. *J. Geophys. Res.*, **98**, 5199–5204.

Bais, A. G., B. G. Gardiner, H. Slaper, H. Slaper, M. Blumthaler, G. Bernhard, R. McKenzie, A. R. Webb, G. Seckmeyer, B. Kjeldstad, T. Koskela, P. J. Kirsch, J. Gröbner, J. B. Kerr, S. Kazadzis, K. Leszczynski, D. Wardle, C. Brogniez, W. Josefsson, D. Gillotay, H. Reinen, P. Weihs, T. Svenœ, P. Eriksen, F. Kuik, and A. Redondas, 2001: The SUSPEN intercomparison of ultraviolet spectroradiometers. *J. Geophys. Res.*, **106**, 12509–12525.

Bass, A. M. and R. J. Paur, 1984: The ultraviolet cross-sections of ozone: 1. measurements. *in C. Zeferos and A. Ghazi (eds.), Proc. Quadrennial Ozone Symp., Halkidiki, Greece*, D. Reidel, Dordrecht, 606–616.

Bernhard, G., C. Booth, J. Ehramjian, and V. Quang, 2003a: *NSF Polar Programs UV Spectroradiometer Network 2000-2001 Operations Report*. Biospherical Instruments Inc., San Diego.

Bernhard, G., C. R. Booth, and J. C. Ehramjian, 2004: Version 2 data of the National Science Foundation's Ultraviolet Radiation Monitoring Network: South Pole. *J. Geophys. Res.*, **109**, D21207, doi:10.1029/2004JD005584.

Bernhard, G., C. R. Booth, and J. C. Ehramjian, 2010: Climatology of ultraviolet radiation at high latitudes derived from measurements of the National Science Foundation's Ultraviolet Spectral Irradiance Monitoring Network. In *UV Radiation in Global Climate Change: Measurements, Modeling and Effects on Ecosystems*, edited by W. Gao, D. L. Schmoldt, and J. R. Slusser, Tsinghua University Press, Beijing and Springer, New York.

Bernhard, G., C. R. Booth, and R. D. McPeters, 2003b: Calculation of total column ozone from global uv spectra at high latitudes. *J. Geophys. Res.*, **108**, doi:10.1029/2003JD003450.

Bernhard, G., C. R. Booths, and J. C. Ehramjian, 2005: Real-time ultraviolet and column ozone from multichannel ultraviolet radiometers deployed in the National Science Foundation's ultraviolet monitoring network. *Opt. Eng.*, **44**, 041011, doi:10.1117/1.1887195.

Bernhard, G. and G. Seckmeyer, 1999: Uncertainty of measurements of spectral solar UV irradiance. *J. Geophys. Res.*, **104**, 14321–14345.

Blumthaler, M., 2004: Quality assurance and quality control methodologies used within the Austrian UV monitoring network. *Radiat. Prot. Dosim.*, **111**, 359–362, doi:10.1093/rpd/nch054.

Bojkov, R., C. Zerefos, D. Balis, I. Ziomas, and A. Bais, 1993: Record low total ozone during northern winter of 1992 and 1993. *Geophys. Res. Lett.*, **20**, 1351–1354, doi:10.1029/93GLO1309.

Booth, C., G. Bernhard, E. Ehramjian, V. Quang, and S. Lynch, 2001: *NSF Polar Programs UV Spectroradiometer Network 1999-2000 Operations Report*. Biospherical Instruments Inc., San Diego.

Brewer, A. W., 1973: A replacement for the Dobson spectrophotometer?. *Pure Appl. Geophys.*, **106-108**, 919–927.

Brühl, C. and P. Crutzen, 1989: On the disproportionate role of tropospheric ozone as a filter against solar UV-B radiation. *Geophys. Res. Lett.*, **16**, 103–106.

Calbó, J., D. Pags, and J.-A. Gonzalez, 2005: Empirical studies of cloud effects on UV radiation: A review. *Rev. Geophys*, **43**, RG2002, doi:10.1029/2004RG000155.

Caldwell, M., L. Camp, C. Warner, and S. D. Flint, 1986: Action spectra and their key role in assessing biological consequences of solar UV-B radiation change. In *Stratospheric Ozone Reduction, Solar Ultraviolet Radiation and Plant Life*, edited by Worrest, R.C. and M.M. Caldwell, Springler-Verlag, Berlin, 87-111.

Caldwell, M., R. Robbrecht, and W. Billings, 1980: A steep latitudinal gradient of solar ultraviolet-B radiation in the Arctic-Alpine life zone. *Ecology*, **61**, 600–611.

Cede, A., M. Blumthaler, E. Luccini, R. D. Piaccentini, and L. Nuñez, 2002a: Effects of clouds on erythemal and total irradiance as derived from data of the Argentine network. *Geophys. Res. Lett.*, **29**, 2223, doi:10.1029/2002GL015708.

Cede, A., E. Luccini, L. Nuñez, R. D. Piacentini, and M. Blumthaler, 2002b: Monitoring of erythemal irradiance in the Argentine ultraviolet network. *J. Geophys. Res.*, **107**, D13207, doi:10.1029/2001JD001206.

Chapman, S., 1930: On ozone and atomic oxygen in the upper atmosphere. *Philosophical Magazine and Journal of Science 10 (September)*, 369–383.

Chubarova, N. Y., A. Y. Yurova, N. A. Krotkov, J. R. Herman, and P. K. Bhartia, 2002: Comparison between ground measurements of UV irradiance 290 to 380 nm and TOMS UV estimates over Moscow for 1979-2000. *Opt. Eng.*, **41**, 3070–3081.

Coakley, J. A., R. D. Cess, and F. B. Yurevich, 1983: The effect of tropospheric aerosols on the earth's radiation budget: a parametrization for climate models. *J. Atmos. Sci.*, **40**, 116–138.

Dahlback, A., 1996: Measurements of biologically effective UV doses, total ozone abundances, and cloud effects with multichannel, moderate bandwidth filter instruments. *Appl. Opt.*, **35**, 6514–6521.

Dahlback, A., N. Gelsor, J. J. Stamnes, and Y. Gjessing, 2007: UV measurements in the 3000–5000 m altitude region in Tibet. *J. Geophys. Res.*, **112**, D09308, doi:10.1029/2006JD007700.

Daumont, D., J. Brion, J. Charbonnier, and J. Malicet, 1992: Ozone UV spectroscopy I: Absorption cross-sections at room temperature. *J. Atmos. Chem.*, **15**, 145–155, doi:10.1007/BF00053756.

De Backer, H., P. Köpke, A. Bais, X. De Cabo, T. Frej, D. Gillotay, C. Haite, A. Heikkilä, A. Kazantzidis, T. Koskela, E. Kyrö, J. Lapeta, B.and Lorente, K. Masson, B. Mayer, H. Plets, A. Redondas, A. Renaud, G. Schauberger, A. Schmalwieser, and K. Vaniceck, 2001: Comparison of measured and modelled UV indices for the assessment of health risks. *Meteorol. Appl.*, **8**, 267–277.

de Gruijl, F. and J. C. van der Leun, 1994: Estimate of the wavelength dependency of ultraviolet carcinogenesis in humans and its relevance to the risk assessment of a stratospheric ozone depletion. *Health Phys.*, **67**, 319–325.

Degünther, M., R. Meerkötter, A. Albold, and G. Seckmeyer, 1998: Case study on the influence of inhomogeneous surface albedo on UV irradiance. *Geophys. Res. Lett.*, **25**, 3587–3590.

den Outer, P. N., H. Slaper, and R. B. Tax, 2005: UV radiation in the Netherlands: Assessing long-term variability and trends in relation to ozone and clouds. *J. Geophys. Res.*, **110**, D02203, doi:10.1029/2004JD004824.

Diaz, A. M., O. E. Garcia, J. P. Diaz, F. J. Expósito, M. P. Utrillas, J. A. Martinez-Lonazo, L. Alados-Arboledas, F. J. Olmo, J. Lorente, V. Cachorro, H. Horvath, A. Labajo, M. Sorribas, J. M. Vilaplana, A. M. Silva, T. Elias, M. Pujadas, A. Rodrigues, and J. A. Gonzàlez, 2007: Aerosol radiative forcing efficiency in the UV region over southeastern Mediterranean: VELETA2002 campaign. *J. Geophys. Res.*, **112**, D06213, doi:10.1029/2006JD007348.

Diaz, S., C. R. Booth, R. Armstrong, C. Brunat, S. Cabrera, C. Camiliãn, C. Casiccia, G. Deferrari, H. Fuenzalida, C. Lovengreen, A. Paladini, J. Pedroni, A. Rosales, H. Zagarese, and M. Vernet, 2005: Multichannel radiometer calibration: a new approach. *Appl. Opt.*, **44**, 5374–5380.

Farman, J., B. Gardiner, and J. Shanklin, 1985: Large losses of total ozone in Antarctica reveal seasonal $CLO_x/NO_x$ interaction. *Nature*, **315**, 207–210.

Frederick, J. and D. Lubin, 1988: The budget of biologically active ultraviolet radiation in the Earth-atmosphere system. *J. Geophys. Res.*, **93**, 3825–3832.

Gao, Z., W. Gao, and N. B. Chang, 2010: Detection of multidecadal changes in UVB and total ozone concentrations over the continental US with NASA

TOMS Data and USDA groundbased measurements. *Remote Sens.*, **2**, 262–277, doi:10.3390/rs2010262.

Garane, K., A. F. Bais, S. Kazadzis, A. Kazantzidis, and C. Meleti, 2006: Monitoring of UV spectral irradiance at Thessaloniki (1990–2005): data re-evaluation and quality control. *Ann. Geophys.*, **24**, 3215–3228.

García, O. E., A. M. Díaz, F. J. Expósito, J. P. Díaz, J. Gröbner, and V. E. Fioletov, 2006: Cloudless aerosol forcing efficiency in the UV region from AERONET and WOUDC databases. *Geophys. Res. Lett.*, **33**, L23803, doi:10.1029/2006GL026794.

Gardiner, B. G. and P. J. Kirsch, 1997: Intercomparison of ultraviolet spectroradiometers, Ispra, 24-25 May 1995. In *Advances in Solar Ultraviolet Spectroradiometry, Air Pollut. Res. Rep. 63*, edited by Webb, A. R., European Commission, Luxembourg, 67-151.

Glandorf, M., A. Arola, A. Bais, and G. Seckmeyer, 2005: Possibilities to detect trends in spectral UV irradiance. *Theor. Appl. Climatol.*, **81**, 33–44, doi:10.1007/s00704-004-0109-9.

Grenfell, T. C., S. G. Warren, and P. C. Mullen, 1994: Reflection of solar radiation by the antarctic snow surface at ultraviolet, visible and near-infrared wavelengths. *J. Geophys. Res.*, **99**, 18,669–18,684.

Gröbner, J., S. J., S. Kazadzis, A. F. Bais, M. Blumthaler, P. Görts, R. Tax, T. Koskela, G. Seckmeyer, A. R. Webb, and D. Rembges, 2005: Traveling reference spectroradiometer for routine quality assurance of spectral solar ultraviolet irradiance measurements. *Appl. Optics*, **44**, 5321–5331.

Gröbner, J. and P. Sperfeld, 2005: Direct traceability of the portable QASUME irradiance standard of the PTB. *Metrologia*, **42**, 134–139.

Haapala, J. K., S. K. Mörsky, S. Saarnio, R. Rinnan, H. Suokanerva, E. Kyrö, K. Latola, P. Martikainen, T. Holopainen, and J. Silvola, 2009: Carbon dioxide balance of a fen ecosystem in northern Finland under elevated UV-B radiation. *Glob. Change Biol.*, **15**, 943–953, doi:doi:10.111/J.1365-2486.2008.01785.x.

Herman, J., P. Bhartia, O. Torres, C. Hsu, C. Seftor, and E. Celarier, 1997: Global distribution of UV-absorbing aerosols from Nimbus 7/TOMS data. *J. Geophys. Res.*, **102**, 16911–16922.

Høiskar, B., R. Haugen, T. Danielsen, A. Kylling, K. Edvardsen, A. Dahlback, B. Johnsen, M. Blumthaler, and J. Schreder, 2003: Multichannel moderate-bandwidth filter instrument for measurement of the ozone-column anount, cloud transmittance, and ultraviolet dose rates. *Appl. Optics*, **42**, 3472–3479.

Huttunen, S., T. Taipale, N. M. Lappalainen, E. Kubin, K. Lakkala, and J. Kaurola, 2005: Environmental specimen bank samples of *Pleurozium schreberi* and *Hylocomium splendens* as indicators of the radiation environment at the surface. *Env. Poll.*, **133**, 315–326.

Johnsen, B., O. Mikkelborg, M. Hannevik, L. Nilsen, G. Saxebøl, and K. Blaasaas, 2002: *The Norwegian UV-monitoring program Period 1995/96 to 2001*. Strålevern Rapport 2002:4, Norwegian Radiation Protection Authority, Østerås.

Josefsson, W., T. Koskela, A. Dahlback, and P. Eriksen, 1994: Spectral sky measurements. In *The Nordic Intercomparison of Ultraviolet and Total Ozone Instruments at Izaña from 24 October to 5 November 1993. Final Report*, edited by Koskela, T., Finnish Meteorological Institute, Meteorological publications No. 27, Helsinki, 73-80.

Josefsson, W. and T. Landelius, 2000: Effect of clouds on UV irradiance: As estimated from cloud amount, cloud type, precipitation, global radiation and sunshine duration. *J. Geophys. Res.*, **105**, 4927–4935.

Kazadzis, S., A. Bais, A. Arola, N. Krotkov, N. Kouremeti, and C. Meleti, 2009: Ozone monitoring instrument spectral UV irradiance products: Comparison with ground based measurements at an urban environment. *Atmos. Chem. Phys.*, **9**, 585–594.

Kazantzidis, A., A. F. Bais, J. Gröbner, J. R. Herman, S. Kazadzis, N. Krotkov, E. Kyrö, P. N. den Outer, K. Garane, P. Görts, K. Lakkala, C. Meleti, H. Slaper, R. B. Tax, T. Turunen, and C. S. Zerefos, 2006: Comparison of satellite-derived UV irradiances with ground-based measurements at four European stations. *J. Geophys. Res.*, **111**, D13207, doi:10.1029/2005JD006672.

Kerr, J. and C. McElroy, 1993: Evidence for large upward trends of ultraviolet-B radiation linked to ozone depletion. *Science*, **262**, 1032–1034.

Kivi, R., E. Kyrö, T. Turunen, T. Ulich, and E. Turunen, 1999: Atmospheric trends above Finland: II.Troposphere and stratosphere. *Geophysica*, **35**, 71–85.

Knudsen, B., N. Larsen, I. Mikkelsen, J.-J. Morcrette, G. Braahten, E. Kyrö, H. Fast, H. Gernand, H. Kanzawa, H. Nakane, V. Dorokhov, V. Yushkov, G. Hansen, M. Gil, and R. Shearman, 1998: Ozone depletion in and below the Arctic vortex for 1997. *Geophys. Res. Lett.*, **25**, 627–630.

Koskela, T., B. Johnsen, A. Bais, W. Josefsson, and H. Slaper, 1997: Spectral sky measurements. In *The Nordic Intercomparison of Ultraviolet and Total Ozone Instruments at Izaña, October 1996. Final Report*, edited by Kjeldstad,B. and Johnsen,B. and Koskela,T., Finnish Meteorological Institute, Meteorological Publications No. 36, Helsinki, 109-148.

Krywult, M., J. Smykla, H. Kinnunen, F. Martz, M.-L. Sutinen, K. Lakkala, and M. Turunen, 2008: Influence of solar UV radiation on the nitrogen metabolism in needles of Scots pine (*Pinus sylvestris* L.). *Env. Poll.*, **156**, 1105–1111, doi:10.1016/j.envpol.2008.04.009.

Kübarsepp, T., P. Kärhä, F. Manoocheri, S. Nevas, L. Ylianttila, and E. Ikonen, 2000: Spectral irradiance measurements of tungsten lamps with filter radiometers in the spectral range 290 nm to 900 nm. *Metrologia*, **37**, 305–312.

Kylling, A., A. Albold, and G. Seckmeyer, 1997: Transmittance of a cloud is wavelength-dependent in the UV-range: Physical interpretation. *Geophys. Res. Lett.*, **24**, 397–400.

Kylling, A., A. Dahlback, and B. Mayer, 2000: The effect of clouds and surface albedo on UV irradiances at a high latitude site. *Geophys. Res. Lett.*, **27**, 1411–1414.

Kyrö, E., P. Taalas, T. Jörgensen, B. Knudsen, F. Stordal, G. Braahten, A. Dahlback, B. Neuber, R.and Krüger, V. Dorokhov, V. Yushkov, V. Rudakov, and A. Torres, 1992: Analysis of the ozone soundings made during the first quarter of 1989 in the Arctic. *J. Geophys. Res.*, **97**, 8083–8091.

Lappalainen, N. M., S. Huttunen, H. Suokanerva, and K. Lakkala, 2010: Seasonal acclimation of the moss *Polytrichum juniperinum* Hedw. to natural and enhanced ultraviolet radiation. *Env. Poll.*, **158**, 891–900, doi:10.1016/j.envpol.2009.09.017.

Leszczynski, K., 2002: *Advances in traceability of solar ultraviolet radiation measurements, Academic Dissertation, University of Helsinki*. STUK-Radiation and Nuclear Safety Authority, Report STUK-A189, October 2002, Helsinki.

Lindfors, A., 2007: *Reconstruction of past UV radiation*. Finnish Meteorological Institute, Contributions No. 67, Helsinki.

Lindfors, A. and A. Arola, 2008: On the wavelength-dependent attenuation of UV radiation by clouds. *Geophys. Res. Lett.*, **35**, L05806, doi:10.1029/2007GL032571.

Lindfors, A., A. Arola, J. Kaurola, P. Taalas, and T. Svenøe, 2003: Long-term erythemal UV doses at Sodankylä estimated using total ozone, sunshine duration, and snow depth. *J. Geophys. Res.*, **108**, 4518, doi:10.1029/2002JD003325.

Lindfors, A., A. Heikkilä, J. Kaurola, T. Koskela, and K. Lakkala, 2009a: Reconstruction of solar spectral surface UV irradiances using radiative transfer simulations. *Photochem. Photobiol.*, **85**, 1233–1239.

Lindfors, A., A. Tanskanen, A. Arola, R. van der A, A. Bais, U. Feister, M. Janouch, W. Josefsson, T. Koskela, K. Lakkala, P. N. den Outer, A. R. D. Smedley, H. Slaper, and A. R. Webb, 2009b: The PROMOTE UV Record: Toward a Global

Satellite-Based Climatology of Surface Ultraviolet Irradiance. *IEEE Journal of Selected Topics in Applied Earth Observation and Remote Sensing*, **2**, 207–212, doi:10.1109/JSTARS.2009.2030876.

Lubin, D. and J. Frederick, 1991: The ultraviolet radiation environment of the Antarctic peninsula: The roles of ozone and cloud cover. *J. Appl. Meteorol.*, **30**, 478–493.

Madronich, S., 1993: The atmosphere and UV-B radiation at ground level. In *Environmental UV Photobiology*, edited by Young et al., Plenum Press, New York.

Madronich, S., 1994: Increases in biologically damaging UV-B radiation due to stratospheric ozone depletion: A brief review. *Arch. Hydrobiol.*, **43**, 17–30.

Madronich, S. and F. R. de Gruijl, 1994: Stratospheric ozone depletion between 1979 and 1992: Implication for biologically active ultraviolet-B radiation and non-melanoma skin cancer incidence. *Photochem. Photobiol.*, **59**, 541–546.

Madronich, S., R. McKenzie, M. Caldwell, and L. Björn, 1995: Changes in ultraviolet radiation reaching the Earth's surface. *Ambio.*, **24**, 143–152.

Martz, F., M. Turunen, R. Julkunen-Tiitto, K. Lakkala, and M.-L. Sutinen, 2009: Effect of the temperature and the exclusion of UVB radiation on the phenolics and iridoids in *Menyanthes trifoliata* L. leaves in the subarctic. *Env. Poll.*, **157**, 3471–3478, doi:10.1016/j.envpol.2009.06.022.

McKenzie, R. L., P. J. Aucamp, A. F. Bais, L. O. Björn, and M. Ilyas, 2007: Changes in biologically-active ultraviolet radiation reaching the Earth's surface. *Photoch. Photobio. Sci.*, **6**, 218–231, doi:10.1039/b700017k.

McKenzie, R. L., J. B. Liley, and L. O. Björn, 2009: UV radiation: Balancing risks and benefits. *Photochem. Photobiol.*, **85**, 88–98, doi:10.1111/j.1751-1097.2008.00400.x.

McKinlay, A. and B. Diffey, 1987: A reference action spectrum for ultraviolet induced erythema in human skin. In *Human Exposure to Ultraviolet Radiation: Risks and Regulations: Proceedings of Seminar Held in Amsterdam, 23-25 March 1987*, edited by Passchler, W.R. and Bosnakovic, B.F.M., Elsevier, Amsterdam, 83-87.

Meinander, O., W. Josefsson, J. Kaurola, T. Koskela, and K. Lakkala, 2003: Spike detection and correction in Brewer spectroradiometer UV spectra. *Opt. Eng.*, **42**, 1812–1819.

Meinander, O., S. Kazadzis, M. Blumthaler, L. Ylianttila, B. Johnsen, K. Lakkala, T. Koskela, and W. Josefsson, 2006: Diurnal discrepancies in spectral solar UV radiation measurements. *Appl. Optics*, **45**, 5346–5357, doi:10.1364/AO.45.005346.

Meinander, O., A. Kontu, K. Lakkala, A. Heikkilä, L. Ylianttila, and M. Toikka, 2008: Diurnal variations in the UV albedo of Artcic snow. *Atmos. Chem. Phys.*, **8**, 6551–6563.

Meinander, O., T. Koskela, K. Lakkala, A. Redondas, C. Torres, E. Cuevas, G. Deferrari, and J. Gröbner, 2004: Antarctic-NILU-UV network linked to QASUME and NSF irradiance scales. In *Proc. of Quadrennial Ozone Symposium QOS 2004, 1-8 June 2004, Kos, Greece*,1128-1129.

Meleti, C., A. F. Bais, S. Kazakzis, N. Kouremeti, K. Garane, and C. Zerefos, 2009: Factors affecting solar ultraviolet irradiance measured since 1990 at Thessaloniki, Greece. *Int. J. Remote Sens.*, **30**, 4167–4179, doi:10.1080/01431160902822864.

Mikkelborg, O., G. Saxebol, and B. Johnsen, 2000: Ultraviolet monitoring in Norway on the Web. *Radiat. Prot. Dosim.*, **91**, 165–167.

Molina, L. and M. Molina, 1986: Absolute absorption cross sections of ozone in the 185-350 nm wavelength range. *J. Geophys. Res.*, **91**, 14501–14508, doi:10.1029/JD091iD13p14501.

Perovich, D. K., T. C. Grenfell, B. Light, and P. V. Hobbs, 2002: Seasonal evolution of the albedo of multiyear Arctic sea ice. *J. Geophys. Res.*, **107**, 8044–8057.

Petters, J. L., V. K. Saxena, J. R. Slusser, B. N. Wenny, and S. Madronich, 2003: Aerosol single scattering albedo retrieved from measurements of surface uv irradiance and a radiative transfer model. *J. Geophys. Res.*, **108**, doi:10.1029/2002JD002360.

Pfeifer, M. T., P. Koepke, and J. Reuder, 2006: Effects of altitude and aerosol on UV radiation. *J. Geophys. Res.*, **111**, D01203, doi:10.1029/2005JD006444.

Redondas, A., C. Torres, O. Meinander, K. Lakkala, R. García, E. Cuevas, H. Ochoa, G. DeFerrari, and S. Díaz, 2008: Antarctic network of lamp-calibrated multichannel radiometers for continuous ozone and UV radiation data. *Atmos. Chem. Phys. Discuss.*, **8**, 3383–3404.

Rex, M., N. Harris, P. Von der Gaathen, R. Lehman, G. Braahten, E. Reimer, A. Beck, M. Chipperfield, R. Alfier, M. Allaart, F. O'Connor, H. Dier, V. Dorokhov, H. Fast, M. Gil, E. Kyrö, Z. Litynska, I. Mikkelsen, M. Molyneux, H. Nakane, J. Notholt, M. Rummukainen, P. Viatte, and J. Wenger, 1997: Prolonged stratospheric ozone loss in the 1995-1996 Arctic winter. *Nature*, **389**, 835–838.

Rinnan, R., A.-M. Nerg, P. Ahtoniemi, H. Suokanerva, T. Holopainen, E. Kyrö, and E. Bååth, 2008: Plant-mediated effects of elevated ultraviolet-B radiation on peat microbial communities of a subarctic mire. *Glob. Change Biol.*, **14**, 925–937, doi:10.1111/j.1365-2486.2008.01544.x.

Rosenfeld, D. and I. M. Lensky, 1998: Satellite-based insights into precipitation formation processes in continental and maritime convective clouds. *B. Am. Meteorol. Soc.*, **79**, 2457–2476.

Sabburg, J. and J. Wong, 2000: The effect of clouds enhancing UVB irradiance at the earth's surface: a one year study. *Geophys. Res. Lett.*, **27**, 3337–3340.

Santer, R., F. Zagolski, and O. Aznay, 2010: Aerosol phase function derived from cimel measurements. *Int. J. Remote Sens.*, **31**, 969–992.

Schmucki, D. A. and Philipona, 2002: Ultraviolet radiation in the Alps: the altitude effect. *Opt. Eng.*, **41**, 3090–3095.

SCI-TEC, 1987: *Brewer Ozone Spectrofotometer, Operational Manual, Maintenance Manual*. SCI-TEC Instruments Inc., Saskatoon, Kanada.

Seckmeyer, G., A. Bais, G. Bernhard, M. Blumthaler, C. Booth, P. Disterhoft, P. Eriksen, R. McKenzie, M. Miyauchi, and C. Roy, 2001: *Instruments to Measure Solar Ultraviolet Radiation,Part 1: Spectral Instruments*. World Meteorological Organization (WMO), Global Atmosphere Watch Report No. 125.

Seckmeyer, G., A. Bais, G. Bernhard, M. Blumthaler, C. R. Booth, K. Lantz, and R. L. McKenzie, 2005: *Instruments to Measure Solar Ultraviolet Radiation, Part 2: Broadband Instruments Measuring Erythemally Weighted Solar Irradiance*. World Meteorological Organization (WMO), Global Atmosphere Watch Report No. 164.

Seckmeyer, G., R. Erb, and A. Albold, 1996: Transmittance of a cloud is wavelength-dependent in the UV range. *Geophys. Res. Lett.*, **23**, 2753–2755.

Seckmeyer, G., M. Glandorf, C. Wichers, R. McKenzie, D. Henriques, F. Carvalho, A. Webb, A.-M. Siani, A. Bais, B. Kjeldstad, C. Brogniez, P. Werle, T. Koskela, K. Lakkala, J. Gröbner, H. Slaper, P. den Outer, and U. Feister, 2008: Europe's darker atmosphere in the UV-B. *Photoch. Photobio. Sci.*, **7**, 925–930, doi:10.1039/b804109a.

Singh, S. and R. Singh, 2004: High-altitude clear-sky direct solar ultraviolet irradiance at Leh and Hanle in the western Himalayas: Observations and model calculations. *J. Geophys. Res.*, **109**, D19201, doi:10.1029/2004JD004854.

Slaper, H., H. A. J. M. Reinen, M. Blumthaler, M. Huber, and F. Kuik, 1995: Comparing ground-level spectrally resolved solar UV measurements using various instruments: A technique resolving effects of wavelength shift and slit width. *Geophys. Res. Lett.*, **22**, 2721–2724.

Smolskaia, I., M. Nunez, and M. Kelvin, 1999: Measurements of erythemal irradiance near Davis Station, Antarctica: Effect of inhomogeneous surface albedo. *Geophys. Res. Lett.*, **26**, 1381–1384.

Taalas, P., E. Kyrö, K. Jokela, T. Koskela, K. Leszczynski, M. Rummukainen, J. Damski, and A. Supperi, 1996: Stratospheric ozone depletion and solar UV radiation in the Arctic and its potential impact on human health in Finland. *Geophysica*, **32**, 127–165.

Tanskanen, A., A. Lindfors, A. Määttä, N. Krotkov, J. Herman, J. Kaurola, T. Koskela, K. Lakkala, V. Fioletov, G. Bernhard, R. McKenzie, Y. Kondo, M. O'Neill, H. Slaper, P. den Outer, A. F. Bais, and J. Tamminen, 2007: Validation of daily erythemal doses from Ozone Monitoring Instrument with ground-based UV measurement data. *J. Geophys. Res.*, **112**, D2S44, doi:10.1029/2007JD008830.

Thorseth, T., B. Kjeldstad, B. Johnsen, M. Blumenthaler, K. Lakkala, and H. Slaper, 2002: Results from the Nordic Intercomparison of ultraviolet spectroradiometers in Sweden 2000. In *Geophysical Research Abstracts. Abstracts of the Contributions of the 27th General Assembly of the European Geophysical Society, 21-26 April 2002*, vol. 4, Nice, France.

Tiiva, P., R. Rinnan, P. Faubert, J. Räsänen, T. Holopainen, E. Kyrö, and J. K. Holopainen, 2007: Isoprene emission from a subarctic peatland under enhanced UV-B radiation. *New Phytol.*, **176**, 346–355, doi:10.1111/j.1469-8137.2007.02164.x.

Turunen, M., M.-L. Sutinen, K. Derome, Y. Norokorpi, and K. Lakkala, 2002: Effects of solar UV radiation on birch and pine seedlings in the sub-Arctic. *Polar Rec.*, **38**, 233–240.

UNEP, 1998: Environmental effects of ozone depletion: 1998 assessment. *J. Photoch. Photobio. B*, **46**, 1–108.

UNEP, 2003: Environmental effects of ozone depletion and its interactions with climate change: 2002 assessment. *Photoch. Photobio. Sci.*, **2**, 1–72.

UNEP, 2007: Environmental effects of ozone depletion and its interactions with climate change: 2006 assessment. *Photoch. Photobio. Sci.*, **6**, 201–332.

Weatherhead, E. C., G. C. Reinsel, G. C. Tiao, X. Meng, D. Choi, W. Cheang, T. Keller, J. DeLuisi, D. J. Wuebbles, J. B. Kerr, A. J. Miller, S. J. Oltmans, and J. E. Frederick, 1998: Factors affecting the detection of trends: Statistical considerations and applications to environmental data. *J. Geophys. Res.*, **103**, 17149–17161.

Webb, A., B. Gardiner, K. Leszczynski, V. Mohnen, P. Johnston, N. Harrison, and D. Bigelow, 2003: *Quality Assurance in Monitoring Solar Ultraviolet Radiation: the State of the Art*. World Meteorological Organization (WMO), Global Atmosphere Watch Report No. 146.

Webb, A., B. Gardiner, T. Martin, K. Leszcynski, J. Metzdorf, and V. Mohnen, 1998: *Guidelines for Site Quality Control of UV Monitoring*. World Meteorological Organization (WMO), Global Atmosphere Watch Report No. 126.

Webb, A. R., L. Kline, and M. F. Holick, 1988: Influence of season and latitude on the cutaneous synthesis of vitamin D3: Exposure to winter sunlight in Boston and Edmonton will not promote vitamin D3 synthesis in human skin. *J. Clin. Endocrinol. Metab.*, **67**, 373–378, doi:10.1210/jcem-67-2-373.

WHO, 2002: *Global Solar UV Index: A Practical Guide*. A joint recommendation of the World Health Organization, World Meteorological Organization, United Nations Environment Programme, and the International Commision on Non-Ionizing Radiation Protection, Geneva, Switzerland.

Winiecki, S. and J. E. Frederick, 2005: Ultraviolet radiation and clouds: Coupling to tropospheric air quality. *J. Geophys. Res.*, **110**, D22202, doi:10.1029/2005JD006199.

WMO, 1990: *Scientific Assessment of Stratospheric ozone: 1989*. World Meteorological Organization (WMO), Global Ozone Research and Monitoring Project–Report No. 20.

WMO, 1994: *Report of the WMO Meeting of Experts on UVB Measurements, Data Quality and Standardisation of UV Indicies*. World Meteorological Organization (WMO), Global Atmosphere Watch Report No. 95.

WMO, 1997: *Report of the WMO-WHO Meeting of Experts on Standardization of UV Indices and their Dissemination to the Public*. World Meteorological Organization (WMO), Global Atmosphere Watch Report No. 127.

WMO, 1999: *Scientific Assessment of Ozone Depletion:1998*. World Meteorological Organization (WMO), Global Ozone Research and Monitoring Project–Report No. 44.

WMO, 2003: *Scientific Assessment of Ozone Depletion:2002*. World Meteorological Organization (WMO), Global Ozone Research and Monitoring Project–Report No. 47.

WMO, 2007: *Scientific Assessment of Ozone Depletion: 2006*. World Meteorological Organization (WMO), Global Ozone Research and Monitoring Project–Report No. 50.

Wuttke, S., G. Seckmeyer, and G. König-Langlo, 2006: Measurements of spectral snow albedo at Neumayer, Antarctica. *Ann. Geophys.*, **24**, 7–21.

Ylianttila, L., R. Visuri, L. Huurto, and K. Jokela, 2005: Evaluation of a single-monochromator diode array spectroradiometer for sunbed UV-radiation measurements. *Photochem. Photobiol.*, **81**, 333–341, doi:10.1562/2004-06-02-RA-184.1.

Young, A., L. Björn, J. Moan, and W. Nultsch, 1993: *Environmental UV Photobiology*. Plenum Press, New York.

Zaratti, F., R. N. Forno, J. García Fuentes, and M. F. Andrade, 2003: Erythemally weighted UV variations at two high-altitude locations. *J. Geophys. Res.*, **108**, 4623, doi:10.1029/2001JD000918.

Zerefos, C., 2002: Long-term ozone and UV variations at Thessaloniki, Greece. *Phys. Chem. Earth Pts. A/B/C*, **27**, 455–460.